POLYMERIZATION AND POLYMER CHARACTERIZATION OF ACETYLENEDICARBOXYLIC ACID MONOPOTASSIUM SALT

A THESIS SUBMITTED TO
THE GRADUATE SCHOOL OF NATURAL AND APPLIED SCIENCES
OF
MIDDLE EAST TECHNICAL UNIVERSITY

BY

ELİF ANAÇOĞLU

IN PARTIAL FULFILMENT OF THE REQUIREMENTS FOR THE DEGREE OF
MASTER OF SCIENCE
IN
POLYMER SCIENCE AND TECHNOLOGY

JANUARY 2005

Approval of the Graduates School of Natural and Applied Sciences

Prof. Dr. Canan ÖZGEN
Director

I certify that this thesis satisfies all the requirements as a thesis for the degree of Master of Sciences

Prof. Dr. Ali USANMAZ
Head of Department

This is to certify that we have read this thesis and that in our opinion it's fully adequate, in scope and quality, as a thesis for the degree of Master of Science in Polymer Science and Technology

Prof. Dr. Ali USANMAZ
(Supervisor)

Examining Commitee in Charge

Prof. Dr. Zuhal KÜÇÜKYAVUZ (CHEM, METU) _____

Prof. Dr. Ali USANMAZ (CHEM, METU) _____

Prof. Dr. Duygu KISAKÜREK (CHEM,METU) _____

Assoc. Prof. Dr. Göknur BAYRAM (CHE, METU) _____

Assoc. Prof. Dr. Metin ZORA (CHEM,METU) _____

I hereby declare that all information in this document has been obtained and presented in accordance with academic rules and ethical conduct. I also declare that, as required by these rules and conduct, I have fully cited and referenced all material and results that are not original to this work.

Name, Last name :

Signature :

ABSTRACT

POLYMERIZATION AND POLYMER CHARACTERIZATION OF ACETYLENEDICARBOXYLIC ACID MONOPOTASSIUM SALT

ANAÇOĞLU, ELİF

M.Sc., Department of Polymer Science and Technology
Supervisor: Prof. Dr. Ali USANMAZ

January 2005, 84 pages

Acetylenedicarboxylic acid monopotassium salt, ADCA-K, was polymerized by radiation induced solid-state and chemical initiator induced solution polymerization methods. Radiation induced solid-state polymerization was carried out by Co-60 γ-radiation at room temperature. The powder polymer obtained was soluble in water but insoluble in common organic solvents. The solution polymerization initiated by benzoylperoxide was carried out in an oil bath at 90°C. The polymer obtained was soluble in water but insoluble in dimethylsulfoxide. In the first stage of the polymerization, H_2O, CO and/or CO_2 gases were evolved and the polymerization was proceeded on the acetylene group.

The polymers obtained were characterized by FT-IR, DSC, TGA-FTIR, NMR and DP-MS methods. The crystal structure effect on polymerization was investigated by X-Ray method. The monomer is monoclinic with a space group of C2/c. The unit cell parameters are a=795.4, b=1192.6, c=591.8 pm and $\beta=105.4^0$. Polymer showed a partial polycrystalline structure. The larger fraction of polymer has identical crystal structure to that of the monomer. Therefore, polymerization takes place a topotactic mechanism.

Keywords: solid-state polymerization, acetylenes, disubstituted acetylenes, space group, radiation polymerization, solution polymerization, hydrogen bonding

ÖZ

ASETİLENDİKARBOKSİLİK ASİT MONOPOTASYUM TUZUNUN POLİMERLEŞTİRİLMESİ VE POLİMER KARAKTERİZASYONU

ANAÇOĞLU, Elif

Y. Lisans, Polimer Bilimi ve Teknolojisi Bölümü

Danışman: Prof. Dr. Ali USANMAZ

Ocak 2005, 84 sayfa

Asetilendikarboksilik asit monopotasyum tuzu, ADCA-K, radyasyonla başlatılan katı-hal ve kimyasal başlatıcılarla başlatılan çözelti polimerizasyonu yöntemleriyle polimerleştirildi. Radyasyonla başlatılan katı haldeki ADCA-K'nın polimerleşmesi Co-60 γ-radyasyonu ile oda sıcaklığında yapıldı. Elde edilen toz polimer suda çözündü ama çoğu organik çözücülerde çözünmedi. Benzoilperoksitle başlatılan çözelti polimerizasyonu yağ banyosunda 90°C'de gerçekleştirildi. Elde edilen polimer suda çözündü, dimetilsulfoksitte çözünmedi. Polimerleşmenin ilk aşamasında, H_2O, CO ve/veya CO_2 gazları çıktı. Daha sonra polimerleşme asetilen bağı üzerinde devam etti.

Elde edilen polimerler, FT-IR, DSC, TGA-FTIR, NMR ve DP-MS metodları ile karakterize edildi. Kristal yapının polimerleşme üzerindeki etkileri X-Işınları yöntemi ile belirlendi. Monomer, uzay grubu C2/c olan monoklinik kristal yapısındadır. Birim hücre parametreleri: a=795.4, b=1192.6, c=591.8 pm ve β=105.4^0'dir. Polimer kısmi polikristal yapı gösterdi. Polimerin büyük kısmı monomerin kristal yapısıyla benzerlik gösterdi. Bu durumda polimorfik bir ürün elde edilmiş oldu. Polimerleşme topotaktik bir mekanizma ile olmaktadır.

Anahtar kelimeler: katı hal polimerleşmesi, asetilen, radyasyanla polimerleştirme, kimyasal başlatıcı, uzay grubu, hidrojen bağı

To my family,

ACKNOWLEDGEMENT

I would to thank most sincerely to Prof.Dr. Ali Usanmaz for his excellent supervision, continued interest and help throughout this work.

I am grateful to my friends Miss Elif Vargün, Bengi Aran and Ayşe E. Aksoy for supporting me morally and helping throughout this thesis and for stimulating discussions and critical suggestions.

Thanks go to Metin Yanık for his help on glass materials and the specialists of the Chemistry department and Central Laboratory especially Necati Özkan and Selda Keskin who help me for the analysis of the samples.

Lastly, I wish to express my deep appreciation to my family for their encouragement, support and comprehension. Without their love, this work could not be accomplished.

TABLE OF CONTENTS

LIST OF TABLES

LIST OF FIGURES

CHAPTER 1

INTRODUCTION

1.1 Solid State Polymerization Induced by Radiation

After discovery of the Ziegler-Natta catalysts, solid-state polymerization studies were encouraged to obtain crystalline polymers. In the solid-state polymerization, the polymer obtained was expected to be crystalline and well oriented, due to small molecular movements in the crystal lattice. It was assumed that, in this case, the polymerization propagates along one of the crystallographic axis of that monomer. However, it was reported that most of the vinyl type monomer gave amorphous polymer in solid-state polymerization. Some monomers with a suitable crystal structure gave crystalline polymer. For example, Usanmaz and Melad[1] reported the topotactic solid-state polymerization of 3-Aminocrotonamide by radiation. The monomer was polymerized by a condensation mechanism and the polymer obtained was crystalline producing NH_3 molecules as a side group. Adler et al[2] studied the polymerization of acrylamide by high-energy radiation. It was expected that a well-oriented crystalline polymer would be obtained, instead an amorphous polymer was obtained which can be explained with the crystal structure effect on solid state polymerization[3]. Also, polymerization continued after removing the sample from

irradiation source, which is called post polymerization. The ESR results showed that in the irradiated mixture of polymer and monomer trapped free radicals were present which can lead to post polymerization if the residual monomer was not separated precisely from polymer.

The solid-state polymerization of diacetylene monomer crystals lead nearly perfect crystals by 1,4-addition reaction. The reaction is promoted by spatial arrangement of the monomer molecules in the crystal matrix. The molecular arrangement was greatly affected by an R group connected to acetylene in the molecule. The reaction can be induced by radiation (γ or UV) or thermally and is usually a topotactic type. However, the reactivity of disubstituted acetylene molecules is very low and no reports were made.[3]

Usanmaz[4] studied on the crystal structure effect in radiation-induced solid-state polymerization of acrylamide. A crystalline polymer was expected to be obtained in a solid-state polymerization because of limited mobility of molecules in the solid matrix. However, polymer was amorphous. When acrylamide is irradiated with X-Ray ions, radical ions and free radicals are generated. These species will react further at proper temperatures to give dimer, polymer, etc. Polymerization of acrylamide proceeds by a two-phase mechanism. After the polymer phase separation, the unpolymerized monomer retains its crystal structure.[4]

1.2 Acetylenes

Solid-state polymerization of acetylene monomer (-C≡C-C≡C-) has been studied from 1970 to recent years[5]. The experiments such as X-Ray diffraction, electron reflection, optical and mechanical properties showed that polymer formed had the same structure with that of monomer. These types of reactions are called topotactic solid-state polymerization. Aoki et al.[6] polymerized acetylene at high pressure. They obtained Raman spectrum of the polymer. The reaction product consisted of two kinds of conjugated polymers, trans-polyacetylene and cis-polyacetylene. Acetylene molecules form planar zigzag patterns in the ab plane of the unit cell. Polymerization reactions accompany opening triple bonds and crosslinking of the polymer molecules. It was expected that polymerization occurred in the bc plane rather than ab plane. There are two possible reaction paths for polymerization in the bc plane. One is linear path running along diagonal of the bc plane (path A). The reaction was proceeded by trans opening of the triple bonds and crosslinking of the adjacent molecules to form a trans polymer. The other is zigzag path, leading to a cis polymer by cis opening of the triple bonds and successive crosslinking reaction of the molecules (path B). The polymerization reaction along path A involves less molecular motions than along path B. The molecules located along path A form a molecular plane inclined somewhat with respect to the b axis of the unit cell. The molecular orientation in this plane is very favorable to a topochemical polymerization. A trans polymer can be formed simply by crosslinking of the adjacent molecules with C-C single bonds. On the other hand, chain propagation along path B involves molecular rotations prior to crosslinking reactions. The axes of the molecules at cis geometry sites along path B are not in the same plane, canting slightly with respect to the backbone plane of the cis polymer to be formed. Therefore, rotations of the molecules into suitable reactive sites in the bc plane are required to form a cis polymer. In solids phase, reactions involving the

least changes in molecular positions are favored. This least motion principle suggests that path A is more preferable to path B for solid-state polymerization. Trout and Badding[7] studied the effect of low temperatures and high pressure on the kinetics and mechanism of solid-state polymerization of acetylene. Low temperatures has to be accompanied with high the pressure to induce reaction, allowing molecules to approach more closely before polymerization begins, also potentially facilitating a topochemical reaction if the initial intermolecular distances in a crystal are too large. Sterically inhibited diacetylenes that do not polymerize at ambient pressure, for example, can be induced to polymerize under high pressure once the distance between carbon atoms is brought below the critical distance of about 4 Å. Hirschfeld and Schmidt[8] observed from topographic studies that the defect free regions of the crystal were uniformly polymerized and was supported by no change in defect density during polymerization. It indicated that dislocations were not the only dominant reaction sites in diacetylene crystals. Thus, solid-state polymerization in diacetylene must be topochemical reaction. This distinguishes it from many other topochemical reactions, which can occur only in the vicinity of lattice defects. They considered a model of solid-state polymerization of diacetylenes. That is a reaction in which diacetylene units are able to undergo 1,4 addition polymerization simply by rotation with centers of gravity on fixed lattice sites. Under such conditions empirical criterion was suggested that reacting carbons must have a separation of less than 0.4 nm in the monomer lattice.

Acetylene and monosubstituted acetylenes can be polymerized to linear polymers by Ziegler Natta catalysts. The substituted acetylene that has been most studied is phenylacetylene. This monomer undergoes polymerization by thermal, radical, cationic, Ziegler-Natta mechanism and transition metal based catalysts. The latter are considered to promote polymerization by a metathesis mechanism similar to metathesis catalysts. The mechanism of polymerization of phenylacetylene and microstructure of its polymers strongly depends on the catalyst, thermal history of

the polymerization reaction and often on the solvent. Keller and Matusiak[9] reported the $Mo(NO)_2(O_2CR)_2$-Lewis acid systems which serve as effective catalysts in the polymerization or cyclotrimerization of monosubstituted acetylenes and concluded that the route of reaction (polymerization or/and cyclotrimerization) depends mainly on the Lewis acid and on the solvent.

1.3 Disubstituted Acetylenes

Some diacetylene monomers crystallize in monoclinic crystal lattices. Polymerization by thermal or photo-initiation results with polydiacetylene chains to grow in a topochemical reaction parallel to the crystal axis. A variety of living polymerization systems using transition metal catalysts has been developed.[10] Substituted acetylenes polymerize by metathesis and insertion mechanisms. The living polymerization of substituted acetylenes has been achieved with Schrock carbenes, $MoOCl_4$-based ternary catalysts, and Rh catalysts. Kubo et al[10] studied the polymerization of aliphatic disubstituted acetylenes by $MoOCl_4$-n-Bu_4Sn-EtOH catalyst giving polymers with narrow MWDs suggesting living polymerization. They concluded that the 5-dodecyne, which has a triple bond in a more inner part, polymerized more slowly than 2-nonyne, their living characters were hardly different. Xu et al[11] studied the transition metal carbonyl catalysts for polymerization of substituted acetylenes. The acetonitrile complexes initiated polymerizations of a variety of mono- and disubstituted acetylenes at room temperature. The halogenated complexes catalyzed polymerizations of phenylacetylene in toluene. The chlorine-containing acetylene monomers were readily polymerized by Mo complexes in nonhalogenated solvents such as toluene, giving polymers with high molecular weights in high yields. Masuda et al[12] reported

that catalysts based on Mo and W (group 6 transition metals) are effective in the polymerization of substituted acetylenes. Monosubstituted acetylenes such as phenylacetylene polymerize with $MoCl_5$ and WCl_6. In contrast, disubstituted acetylenes such as 1-phenyl-1-propyne and 2-hexyne do not polymerize with these catalysts alone, whereas they do polymerize in the presence of suitable organometallic cocatalysts. $NbCl_5$ and $TaCl_5$, group 5 transition metal chlorides work as excellent catalysts for the polymerization of disubstituted acetylenes. The organometallic cocatalysts exerted various effects such as the formation of polymerization species, the acceleration of polymerization, the increase of polymer molecular weight, and the formation of cyclotrimerization species, depending on the kind of the monomer.

Masuda et al[13] also studied on the polymerization of propiolic acid and its derivatives by $MoCl_5$-based catalysts. The polymer formed was a water-soluble powder having a low molecular weight. Derivatives of propiolic acid (methyl propiolate, acetylenedicarboxylic acid, and phenylpropiolic acid) also produced colored powdery polymers in the presence of $MoCl_5$-based catalysts. Yamaguchi and Osakada[14] reported that the ruthenium (III) complex catalyzes the polymerization of propiolic acid to give a mixture of poly(propiolic acid) and also the polymerization of acetylenedicarboxylic acid and propargyl alcohol to give the corresponding poly(acetylene) derivatives.

1.4 Acetylenedicarboxylic acid (ADCA)

Monocarboxylic acids R-CO_2H, which are either nonchiral or racemic, almost invariably form cyclic hydrogen-bonded pairs. If the R group is small, the molecules may interlink by single O-H---O bonds to form a chain motif in which the O-H---O (carboxyl) bond is almost linear, the C=O---(H)O angle ≅ 130°, and the O-H proton donor lies in the plane of the carbonyl system O=C<, to which it is hydrogen-bonded.[15] Monocarboxylic acids with chiral residues and which are enantiometric show some tendency to form a hydrogen-bonded chain motif along a twofold screw axis. The angular geometry of this O-H---O bond shows considerable variation and seems to be dependent upon the van der Waals contacts between the R groups along the hydrogen-bonded chain. Dicarboxylic acids HO_2C-R-CO_2H form extended chains, the carboxyl groups being interlinked by O-H---O bonds into cyclic pairs[15]. This type of arrangement is adopted, almost without exception, for all types of R groups. Carboxylic acids, in which the intramolecular environments of the two carboxyl O atoms are identical, may show orientational disorder of the carboxyl group in the crystal. This depends on the intermolecular environment of the carboxyl dimer. Carboxylic acids also form interplanar contact via an antiparallel arrangement of C-O bonds which may be either C=O or C-OH bonds or a disordered combination. Intramolecular forces probably favor the synplanar C=C-C=O conformation in α,β-unsaturated acids R-CH=CH-CO_2H.[15] The antiplanar C=C-C=O form may be induced by intermolecular forces. Orientational disorder between the syn- and antiplanar C=C-C=O conformations may be induced by the stacking forces of the carboxyl dimers. The observed antiplanar C=C-C=O conformation in a number of acids has been associated with a motif containing a lateral C-H---O (carbonyl) contact ≅3.5 Å.[15] The few known crystal structures of carboxylic acids containing an acetylenic C-H proton donor have not shown acetylenic C-H---O (carbonyl) interactions, which are strikingly short. The minimum van der Waals

distance between carboxyl O atoms appears to be dependent upon their direction of approach. Hydroxyl O atoms which make contact so that C-O(H) bonds are almost collinear, and may approach each other to within 2.9 Å. Carbonyl and hydroxyl O atoms which are arranged so that their electron lone-pair lobes are directed at each other do not make contact less than 3.5A.[15]

It is of interest that anhydrous acetylenedicarboxylic acid forms the type of hydrogen bonding shown in the Figure 1.1 by virtue of the dihedral angle of 58° between the planes of the two carboxyl groups. Crystals are monoclinic, space group $P2_1/n$, Z=4, having cell parameters a=14.894, b=6.420, c=4.862Å, β=90.90°. Nonplanarity of ADCA is induced by crystal forces.[16]

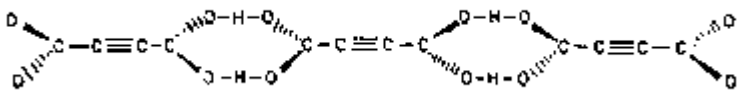

Figure 1.1. Packing symmetry of ADCA

The crystal structure of ADCA show a measure of packing symmetry about the carboxyl O atoms which perhaps accounts for the disorder as indicated by the C-O lengths (1.261, 1.248, 1.262, 1.244A).[15] Furthermore, the IR spectrum of crystalline anhydrous ADCA shows the band at 1700 cm^{-1}, due to the carbonyl-stretching mode. From the disorder of the carboxyl dimers that the intermolecular separation of the two carboxyl groups by the acetylene bond is sufficient to permit the existence of both conformers shown in Figure 1.2.[15]

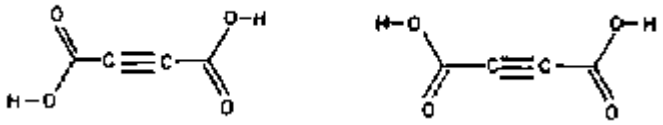

Figure 1.2. Carbonyl stretching mode of ADCA

Usanmaz and Alturk[17] studied the radiation induced solid-state polymerization of ADCA. They investigated the crystal structure of monomer and polymer by XRD method. They concluded that monomer and crystalline polymer had similar cell parameters meaning that the polymerization follows a topotactic mechanism by evolution of CO and CO_2 in the monomer molecule. Cataldo[18] reported the production of CO, CO_2 and soluble polyynes but no free acetylene in the anodic oxidation of this compound. Allan et al[19] studied the thermal properties of the salts of acetylenedicarboxylic acid with iron (II), cobalt (II), nickel (II), copper (II) and zinc (II) in aqueous solution which shows loss of water of crystallization followed by organic ligand to give the metal oxide.

1.5 Salts of Acetylenedicarboxylic Acid

Acid salts of acetylenedicarboxylic acid form polymeric structures with strong hydrogen bonds. The O---O distances lie in the range of 2.43-2.47 Å.[20] They are classified into two groups. In one group, the two carboxyl groups involved in the short hydrogen bond are related by crystallographic symmetry elements (Type A and A_2 for acid salts of carboxylic and dicarboxylic acid respectively). In the other group the carboxylic acid and carboxylate groups are crystallographically nonequivalent and referred as Type B and B_2 salts. The hydrogen bond lengths in type A and A_2 salts are generally shorter than 2.48Å, while the lengths in type B and B_2 salts cover the range up to 2.6Å.[21] Mattes et al[20] reported the structure of lithium hydrogen acetylenedicarboxylate monohydrate (LiHADC). The anions are connected by strong hydrogen bonds. As a small cation, lithium usually favors very short hydrogen bonds in similar compounds. This might be explained by the unfavorable packing requirements of the stiff acetylenic backbone together with the presence of rather strong polar forces in the Li coordination sphere. The Li ion and the water molecule are situated between the pairs of anionic chains. Gupta et al[22] investigated the crystal structure of cesium salt of acetylenedicarboxylic acid, $CsHC_4O_4.H_2O$ using X-Ray single crystal data for studying the hydrogen bonded solids. The structure consists of extensive chains of acetylenedicarboxylic acid residues. Parallel extensive chains of molecules are crosslinked by hydrogen bonds via the water molecules. The crystal structure is being refined to locate the hydrogen atoms, which probably are so fixed as to give short symmetrical hydrogen bonds of 2.44 Å in the structure. Leban et al[23] studied the crystal structure of α-form of potassium hydrogen acetylenedicarboxylate (ADCA-K). The potassium salt of acetylenedicarboxylic acid is of special interest because it contains only one hydrogen atom likely to be involved in O···H···O bonding which should simplify the interpretation of its spectrum. Its IR spectrum is of Hadži's type (ii), which

suggested that the crystal structure would probably be of the symmetrical Type A_2. It consists of hydrogen anions, symmetrical about a two-fold axis of the crystal, linked into infinite chains by very short hydrogen bonds, which lie across two-fold axes of another set. The crystal symmetry elements at the center of the O···H···O bond and of the C≡C bond are both diagonal axes. Blain et al[24] studied the β-form of Rubidium Hydrogen Acetylenedicarboxylate and compared with the isomorphous α-forms of the potassium and rubidium salts. Despite the difference of crystal symmetry the structures found for the hydrogen-anion and for the environment of the cation are very similar to those in the α-form. The hydrogen bond, unsymmetrical in the β-form, which links the anions into infinite chains, has O···O 2.464 Å. The environments of the cations are also alike. The Rb ion in the β-form is in a general position, surrounded by six independent oxygen atoms. Whereas a crystallographic two-fold axis passes through K^+ (in α), Rb^+ (in β) has only a local pseudo-axis. The dihedral angle between the planes is 61°, which differs significantly from the corresponding dihedral angle in α-KH (adc) (66°). Rotation about the acetylenic chain is almost free in the gaseous state.

Hohn et al[25] reported the synthesis and crystal structure of $Sr[C_2(COO)_2]$, the first anhydrous salt of the acetylenedicarboxylate dianion, which shows a surprising thermal stability up to 750K and a small negative thermal expansion between 30K and 280K. This stability is caused by a close packing of the $C_2(COO)_2^{-2}$ anions in the highly symmetric tetragonal crystal structure of $Sr[C_2(COO)_2]$, which does not contain additional water molecules. The decomposition is accompanied by a mass loss of approximately 12%, which is probably due to the loss of CO molecule. The resulting residue is amorphous to X-Rays. Ruschewitz et al[26] studied the two co-ordination polymers of the acetylenedicarboxylate dianion, $Co(C_2(COO)_2)(H_2O)_4.2H_2O$ and $Co(C_2(COO)_2)(H_2O)_2$. In the solid-state structure cobalt is octahedrally surrounded by four water molecules and two oxygen atoms of the

carboxylate anions. These octahedra are connected to chains by the dicarboxylates. In the crystal structure of the first cadmium salt of acetylenedicarboxylic acid $[Cd(C_2(COO)_2)\ (H_2O)_3].H_2O$, the Cd^{II} atom is surrounded by two bidentate carboxylate groups and three water molecules, thus forming a sevenfold coordination polyhedron with all atoms located on general sites. These polyhedra are connected by the bifunctional acetylenedicarboxylate ligands, forming zigzag chains. Hydrogen bonds, which involve the non-coordinated water molecule, connect these chains to form a three-dimensional framework.[27] Skoulika et al[28] reported the crystal structure and solid-state reactivity of a Cd(II) polymeric complex with acetylenedicarboxylic acid. The structure is made up of metal-organic chains linked by hydrogen bonds to form channels along the b axis. The carbon-carbon triple bonds are in close proximity (3.27Å) along the a axis. This induces, upon heating, polymerization with formation of conjugated polycarboxylic chains. If the ligand-ligand distance may be further decreased within the reaction distance (<4.20Å), by employing unsaturated dicarboxylic acids. In this case, "in situ" polymerization would be possible either by heating or by using ionizing radiation. Ruschewitz et al[29] reported the crystal structure of the first copper complex of acetylenedicarboxylic acid $[Cu(C_2(COO)_2)\ (H_2O)_3].H_2O$. Two monodentate carboxylate groups in trans positions and three water molecules coordinates the Cu^{II} ion which forms a fivefold coordination polyhedron that can be described as a distorted square pyramid. Three-dimensional framework is formed by hydrogen bonds containing the non-coordinated water molecule. They also reported the crystal structure of two co-ordination polymers of the acetylenedicarboxylate dianion, $Ni(C_2(COO)_2)(H_2O)_4.2H_2O$ and $Ni(C_2(COO)_2)\ (H_2O)_2$. In the solid-state structure nickel is octahedrally surrounded by four water molecules and two oxygen atoms of the carboxylate anions. These octahedra are connected to chains by the dicarboxylates.[30] Leban and Rupnik[31] studied the structure of guanidium hydrogen acetylenedicarboxylate. The crystal structure consists of infinite chains of hydrogen acetylenedicarboxylate residues linked together by planar guanidium cations. There

are O···H···O hydrogen bonds within the chain and N-H···O bonds between the chains and guanidium cations. McCormick et al[32] reported the copper acetylenedicarboxylate system. The copper complex decomposes explosively when heated rapidly, providing a black phase consisting of carbon and copper that may be described as copper acetylide. It was doped with iodine having a good conductivity.

1.6 Potassium Salt of Acetylenedicarboxylic Acid

The crystal structure of ADCA-K (Figure 1.3) was investigated by Leban et al.[23] The compound crystallizes with Z=4 in a cell with a=7.954, b= 11.926, c=5.918 Å, β=105.4°, space group C2/c. The structure is monoclinic and consists of one-dimensional chains of carboxylate anions linked at both ends by short ionic hydrogen bonds. The hydrogen bond length, i.e. the distance between the two oxygen atoms, of ADCA-K is 2.445 Å. It is very short compared with those of the hydrogen-bonded crystals reported so far and are less than the critical value, 2.5 Å, below which the proton potential is considered to be a single well.

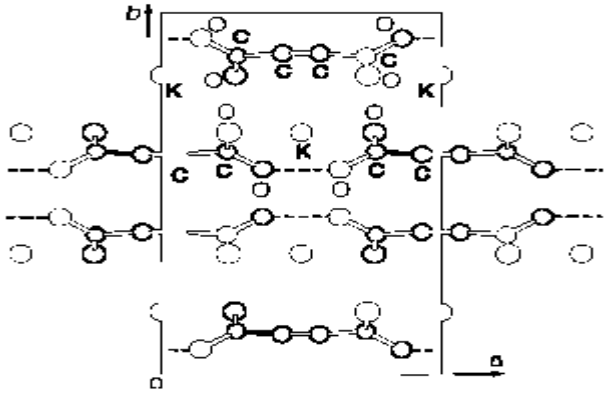

Figure 1.3 Molecular Packing of ADCA-K

Sekikawa et al[33] investigated the potassium salt of acetylenedicarboxylic acid with strong ionic hydrogen bond between the two carboxyl groups by infrared spectroscopy from the mid- to far-IR region to elucidate the role of the charge transfer in the hydrogen bonds under hydrostatic pressure and at various temperatures. They concluded that the absorption coefficient of the higher $\nu_{C=O}$, which is sensitive to the hydrogen bond length and temperature. The absorption coefficient of the higher $\nu_{C=O}$ was enhanced with decreasing hydrogen bond length by the electron rearrangement due to the charge transfer. The higher $\nu_{C=O}$ also showed broadening of the line width with an increase in temperature due to the anharmonic coupling caused by the charge transfer. The temperature dependence of ^2H Nuclear Quadrupole interaction in very short hydrogen bonds in some organic acidic salt crystals was reported. The temperature coefficient decreases with increase in the O···O distance in the hydrogen bond. The ^2H NMR spectral line shape does not undergo any significant change on heating, but the line width increases remarkably with increasing in temperature.[34] Cataldo made a new approach to the anodic decarboxylation of unsaturated dicarboxylic acids. Anodic oxidation of acetylenedicarboxylic acid produces only a mixture of carbon dioxide, carbon monoxide and soluble polyynes; no free acetylene has been detected.[18]

1.7 Aim of The Study

In this study, ADCA-K is polymerized by radiation induced solid-state and chemical initiator induced solution polymerization methods. The crystal structure effect on polymerization is investigated by X-Ray method and the nature of structure of monomer and polymers are determined by FT-IR and NMR spectra. The thermal properties of the monomer and the polymer are studied by DSC, TGA and MS analysis.

CHAPTER 2

EXPERIMENTAL

2.1 MATERIALS

2.1.1 Monomer

Acetylenedicarboxylic acid monopotassium salt (Aldrich Chemical Co.) was used as monomer recrystallized in water-acetonitrile (1;1 v/v). The chemical structure of the monomer is given below.

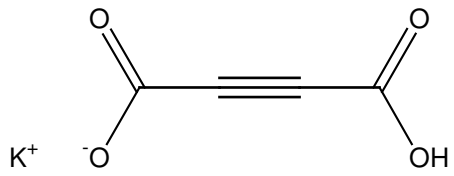

2.1.2 Solvent

Dimethylsulfoxide (DMSO) obtained from Atabay Kimya Sanayi was used as solvent. It was purified by distillation.

2.1.3 Initiator

Benzoylperoxide (BPO) obtained from Merck was used as initiator for the solution polymerization. The chemical structure is given below.

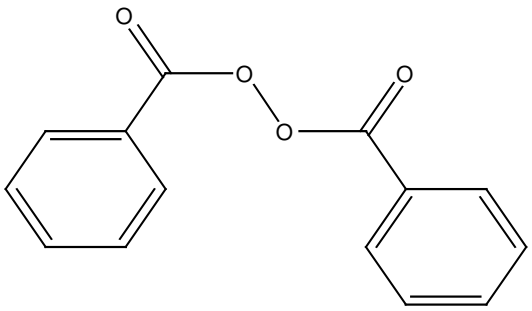

2.2 INSTRUMENTATION

2.2.1 Co-60 γ-Ray Source

The used radiation source is 220 Model Gamma Cell of Atomic Energy of Canada Limited Co. Cobalt is in the form of rigid cylinder rods and 24 Co rods are put around hollow cylindrical chamber. Samples to be irradiated were hold in a cylinder chamber that could be automatically lowered to the irradiation source. The dose rate of radiation is 0.015 Mrad/h.

2.2.2 Polymerization Tubes

The tubes used for polymerization of ADCA-K were 1-1.5 cm in diameter and 20-25 cm in length Pyrex tubes.

2.2.3 X-Ray Powder Diffractometer

X-Ray powder diffraction patterns were taken on Rigaku Miniflex XRD with Cu Kα (30 kV, 15 mA) X-rays.

2.2.4 Infrared Spectrometer

IR spectra of monomer and polymers were taken from KBr pellets by using Perkin Elmer-Spectrum-One FT-IR Spectrometer. The data was processed by the OMNIC computer program.

2.2.5 Differential Scanning Calorimeter

The thermal analyses of the samples were recorded by Dupont Thermal Analyst 2000 Diffential Scanning Calorimeter 910S. Heating rate was 10°C/min from room temperature to 300°C under nitrogen gas atmosphere.

2.2.6 Direct Pyrolysis-Mass Spectrometry

The mass spectrometer used for direct pyrolysis experiment was Balzers QMG 311 quadrupole mass spectrometer via a personnel computer for the control of the MS data acquisition and analysis.

2.2.7 Thermal Gravimetric Analysis

The thermal behavior of monomer and polymer was observed by Perkin Elmer Pyris 1 TGA & Spectrum 1 FT-IR Spectrometer.

2.2.8 Nuclear Magnetic Resonance Spectrometer

The liquid state ^{1}H and ^{13}C spectra of monomer and polymer were taken on Bruker High Resolution Nuclear Magnetic Resonance Spectrometer, Ultrashield 400 MHz Digital NMR. The solid state spectra were taken on Bruker High Power Superconducting Ultrashield 300 MHz FT. NMR with 4mm MAS probe for ^{1}H and ^{13}C Cross Polarization spectra.

2.3 PROCEDURE

2.3.1 Radiation Induced Solid State Polymerization of ADCA-K

About 1-2 gr of monomer samples were put into the irradiation tubes which, were evacuated on high vacuum system then sealed, They were irradiated by γ rays for desired period of time. After irradiation, tubes were broken open; samples were dissolved in small amount of DMSO, which is solvent for monomer and nonsolvent for polymer. The polymer was filtered and dried to constant weight. The percent conversion of the monomer to the polymer was calculated.

2.3.2 Solution Polymerization of ADCA-K

A 0.055M 3 mL DMSO solution of monomer were prepared and 0.001 gr (0.0014M) of BPO added. The tubes were evacuated on high vacuum system and placed in an oil bath at 90°C for the desired time. The polymer was precipitated and removed by centrifugation. The samples were vacuum dried at 50°C to constant weight. The polymerization was also repeated with solutions of 0.0275M monomer and 0.0014M initiator; 0.055M monomer and 0.0028M initiator. The conversions were calculated gravimetrically.

CHAPTER 3

RESULTS AND DISCUSSION

3.1 Polymerization of ADCA-K

ADCA-K was polymerized by solid state and solution polymerization techniques. Solid-state polymerization of ADCA-K was carried out by Co–60 γ-radiation at room temperature. The sample changed color from white to dark brown. It is soluble in distilled water, but insoluble in DMSO. The percent conversions and corresponding irradiation times are tabulated in Table 3.1. The plot of percent conversion against irradiation time is given in Figure 3.1. The solid-state polymerization (Figure 3.1) of ADCA-K follows two-stage kinetics. In the first stage, the rate is high up to 28% conversion. Then, the rate becomes almost constant for about 100 days of irradiation, and then increase again up 42%. The two-stage polymerization is most probably related to the changes in the crystal structure with evolution of crystal water and splitting of CO and/or CO_2 during the polymerization. The polymerization is slow since the monomer molecules have to be in locations that will be suitable for addition reaction. If the active end of monomer molecules is more than Van der Waals distance apart from each other, the addition will not be

possible. In this case, the energy has to be given to change the location of molecule by overcoming lattice energy and put the monomer in more favorable position for addition reaction. Since the dose rate of irradiation source is very low to get a better result, very long time of irradiation is needed. The structure effect will be given in section of XRD results.

Table 3.1 The percent conversion vs. time for solid-state polymerization of ADCA-K

Time (day)	% Conversion
120	15.6
151	19.4
173	24.8
186	25.7
198	27.2
226	27.6
346	28.0
375	32.2
387	38.1
412	41.8

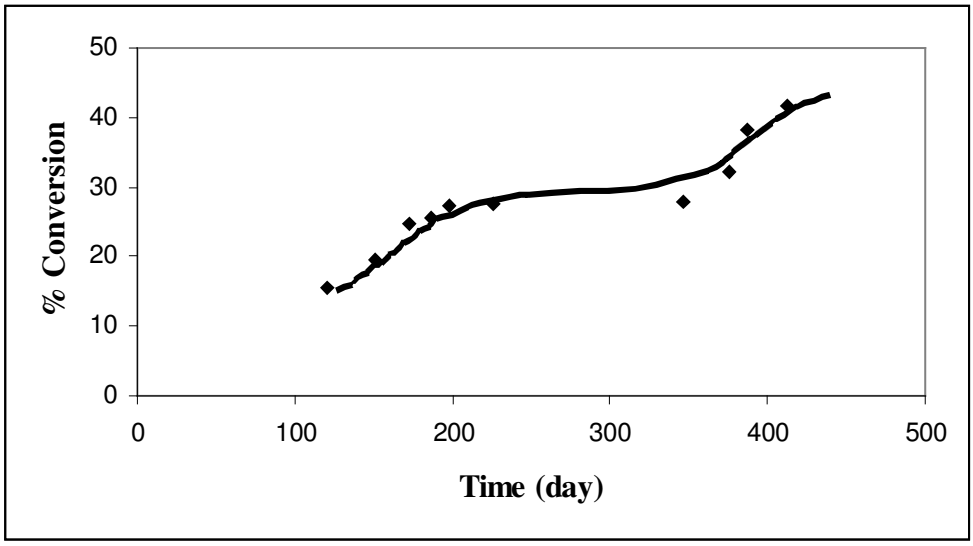

Figure 3.1 % Conversion vs. time graph for solid-state polymerization of ADCA-K

Radical initiated solution (0.055M monomer and 0.0014M initiator) polymerization of ADCA-K was done at 90°C in an oil bath. The results are tabulated in Table 3.2 and the percent conversions against time are plotted in Figure 3.2. The polymerization is highly exothermic and the heat of polymerization could not be dissipated from the viscous medium.

Table 3.2 The percent conversion vs. time

for solution polymerization of ADCA-K

Time (hour)	% Conversion
2.5	25.4
24	39.0
45	40.7
48	47.3
69.5	52.6
72	65.8
96	51.2
120	51.9
144	62.0
264	94.9

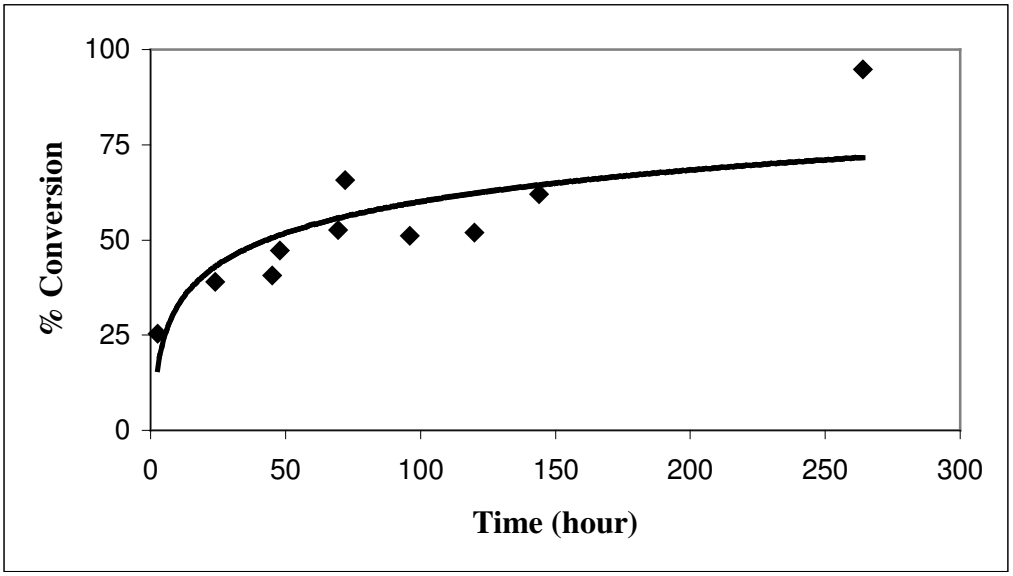

Figure 3.2 % Conversion vs time graph for 0.055M monomer and 0.0014M initiator

The kinetic of polymerization were evaluated for different concentrations of monomer and initiator. The percent conversions versus time for 0.0275M monomer and 0.0014M initiator are given in Table 3.3 and plotted against time in Figure 3.3, respectively. The data are less scattered and percent conversion gives a smoother change. This may be due to the formation of more homogenous solution at lower monomer concentration. Since the polymer precipitate when reaching to a certain molecular weight, the polymerization in a two-phase system becomes more complicated. The molecular weight determination would be very useful to explain both the kinetic and mechanism of polymerization. However, polymer is not reasonably soluble in any solvent for determination of molecular weight.

Table 3.3 The percent conversion vs. time for solution polymerization of ADCA-K

Time (hour)	% Conversion
1	35.2
24	38.6
48	48.8
72	50.8
96	57.4
144	59.4
192	60.7
216	62.0
240	60.0
264	62.4

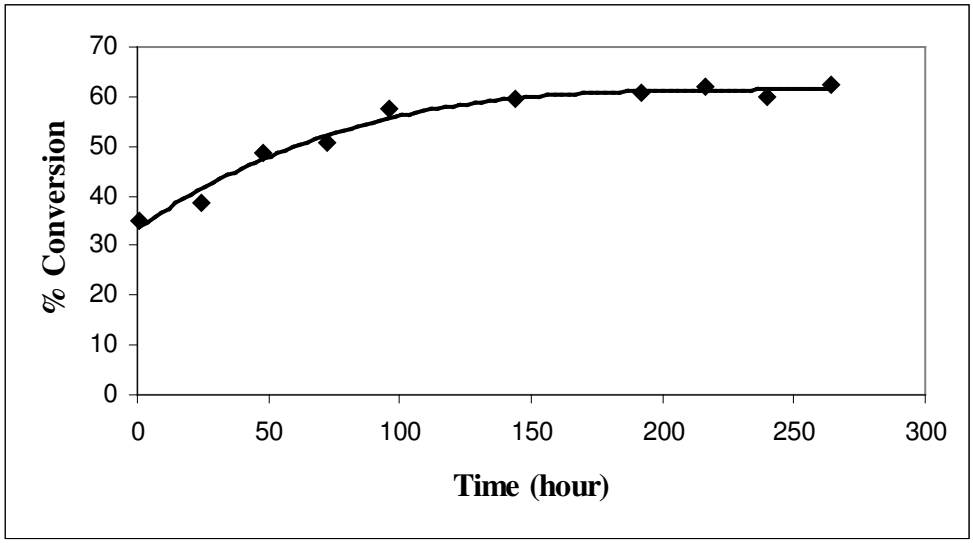

Figure 3.3 % Conversion vs time graph for 0.0275M monomer and 0.0014M initiator

The percent conversion against polymerization time are tabulated in Table 3.4 and plotted in Figure 3.4 for 0.055M monomer and 0.0028M initiator. The polymerization shows the same trend of polymerization with small differences in the values of percent conversion against time.

Table 3.4 The percent conversion vs. time

for solution polymerization of ADCA-K

Time (hour)	% Conversion
2	38.6
24	38.4
48	54.0
72	52.0
120	54.6
192	57.4
217	62.5

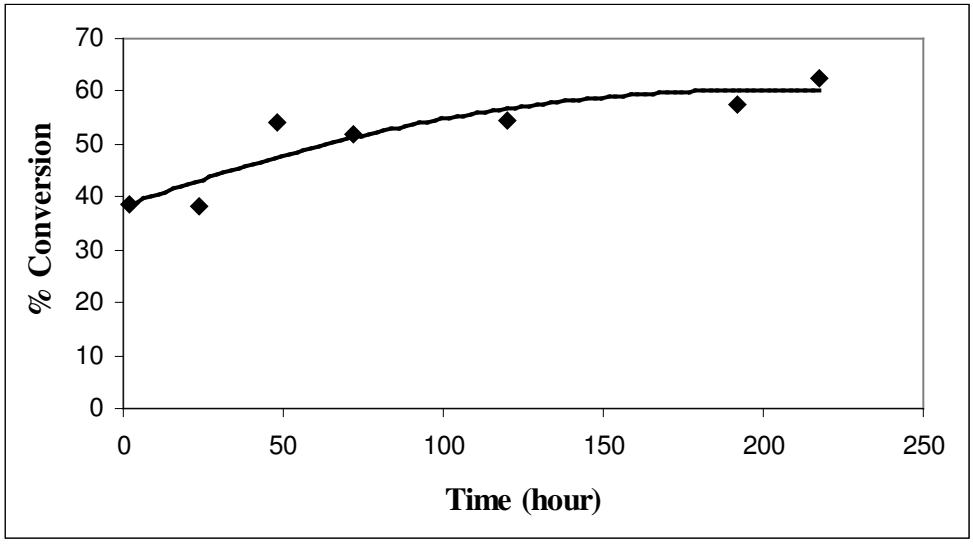

Figure 3.4 % Conversion vs time graph for 0.055M monomer and 0.0028M initiator

3.2 Infrared Spectral Investigation

The FT-IR spectra of monomer is given in Figure 3.5a. In this spectrum, a broad peak shows the strong hydrogen bonding and the crystal water molecules in the monomer. This is also the hydrogen bonding dimerization of monomer, which makes the structure symmetric and dipole moment zero. Therefore the -C≡C- peak cannot be observed in this spectrum. The C=O stretching is observed at 1665 cm^{-1} and C-O stretching at 1291 cm^{-1}. In order to remove the crystal water and break the dimmer structure, the monomer was heated up to 200^0C. At high rate of heating between 120-130^0C, the gas evaluation was instantaneous and explosive. However, slow heating (about 1^0C/min) gave no explosion. The FTIR spectrum of monomer at 100°C is given in Figure 3.5b. The OH vibration is observed at 3260-3700 cm^{-1}, the overlapped C=O and C=C stretching is splitted at 1665 and 1618 cm^{-1}, respectively. The ester C-O stretching is observed at 1030 cm^{-1}. When the temperature is increased to 150°C (Figure 3.5c), a broad OH vibration is observed at 3350 cm^{-1}. This shows the hydrogen bonding and retention of dimerization. Crystal water is removed, but -C≡C- peak is still not observed due to symmetrical structure. At 190^0C (Figure 3.5d), FTIR spectrum showed more changes. Weak -C≡C- and corresponding conjugates peak at 2300-2500 cm^{-1} are observed. Cyclization can also be predicted from peaks in the region of 600 to 1400 cm^{-1}.

The FTIR obtained from solid-state polymerization is given in Figure 3.6, Sharp OH vibration is at 3700 cm^{-1} and 3784 cm^{-1}, -C≡C- peak at 2359 cm^{-1}, C=O at 1619 cm^{-1}. After $C0_2$/CO evolution, side group cyclization takes place and CH_2 peak at 1369 cm^{-1} are observed. Cyclic etheric C-O- stretching is observed at about 985 cm^{-1}. In the FTIR spectrum of polymer of solution polymerization (Figure 3.7), CH bending is observed at 2967 cm^{-1}, C=O and CH_2 stretching at 1631 cm^{-1} and 1403 cm^{-1}, respectively and the cyclic etheric carbon stretching at about 1000 cm^{-1}.

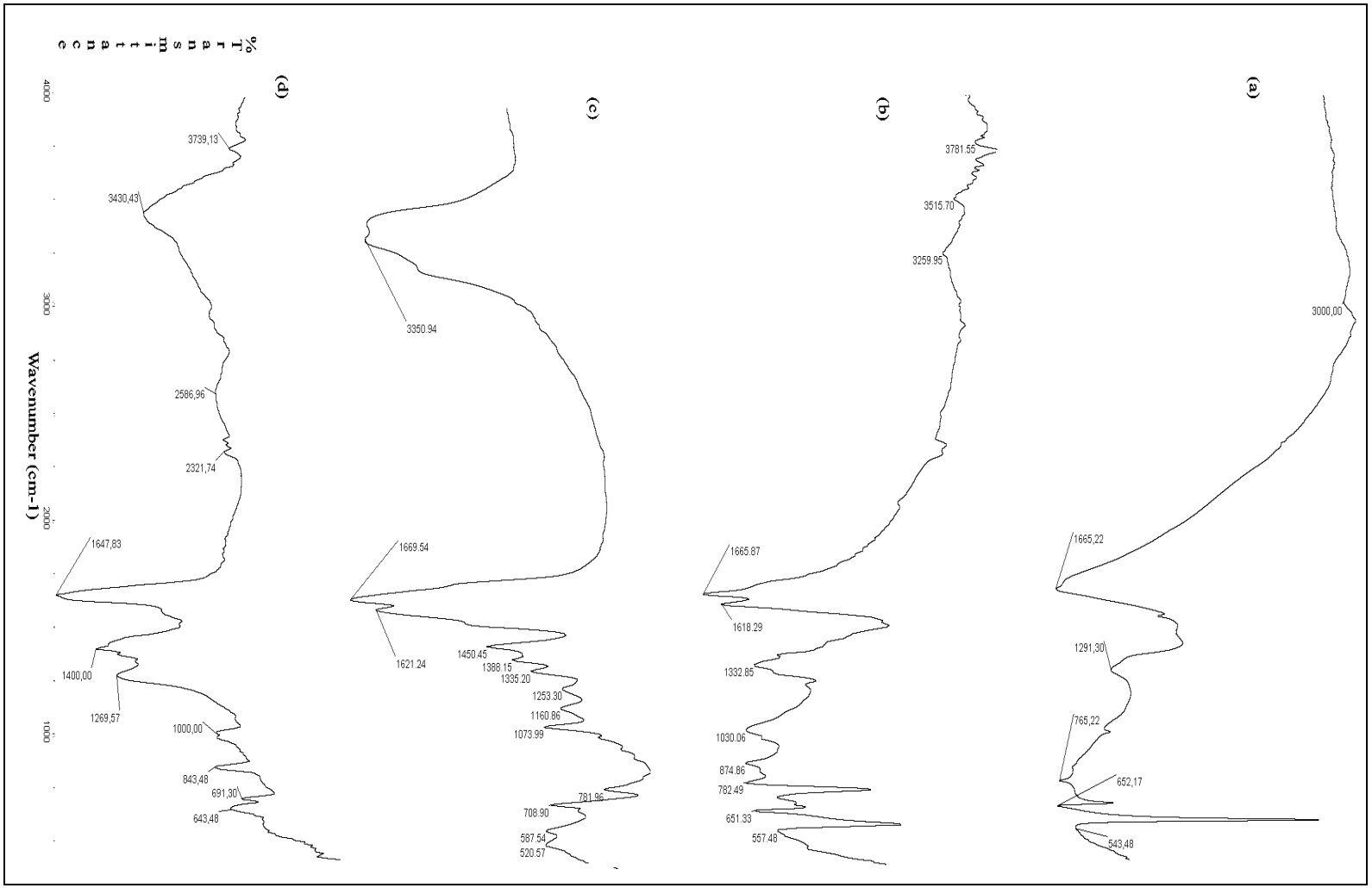

Figure 3.5 FT-IR spectrum of a) monomer; b) monomer at 100°C; c) monomer at 150°C; d) monomer at 190°C

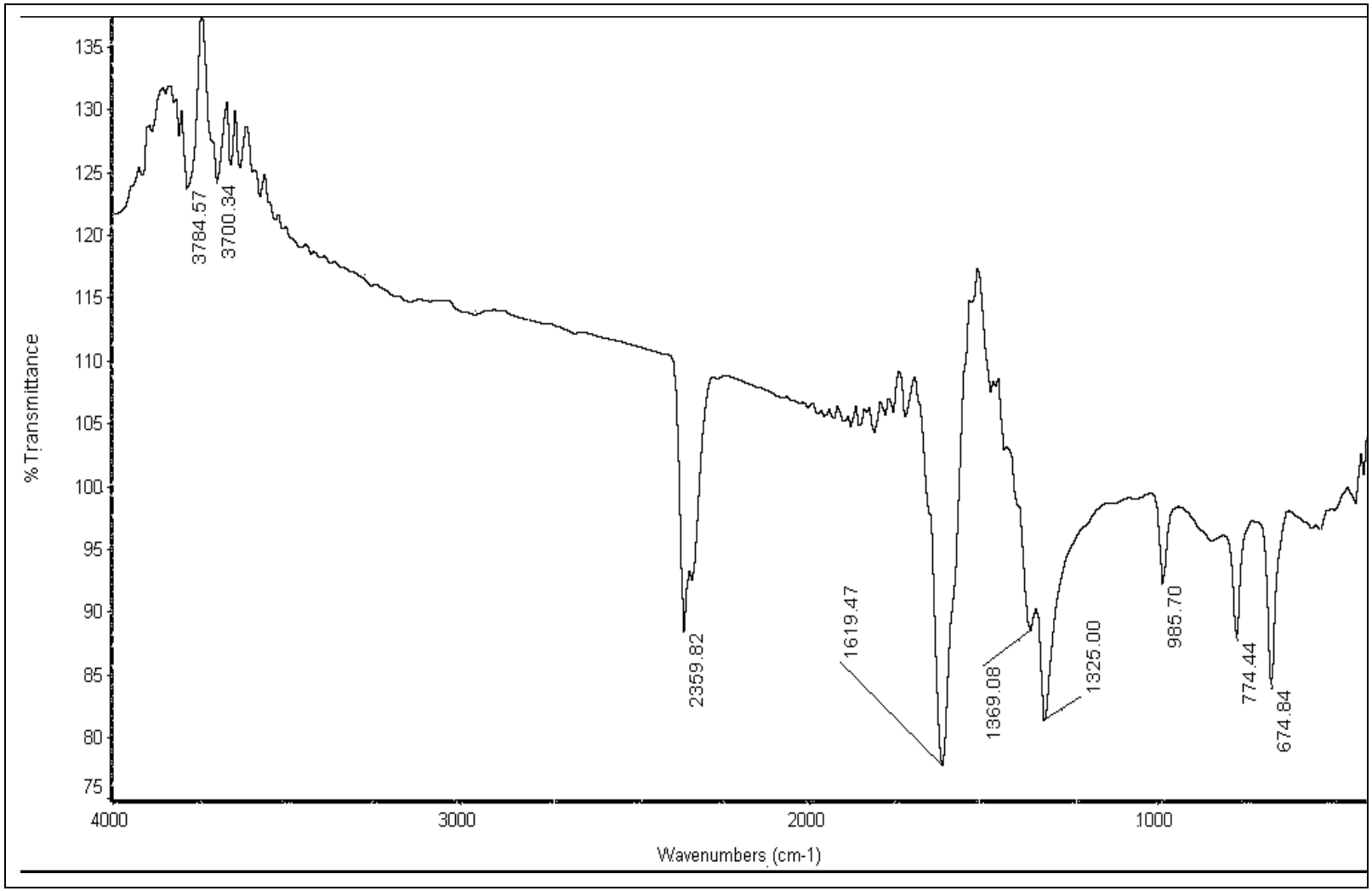

Figure 3.6 FT-IR spectrum of polymer obtained by solid-state polymerization

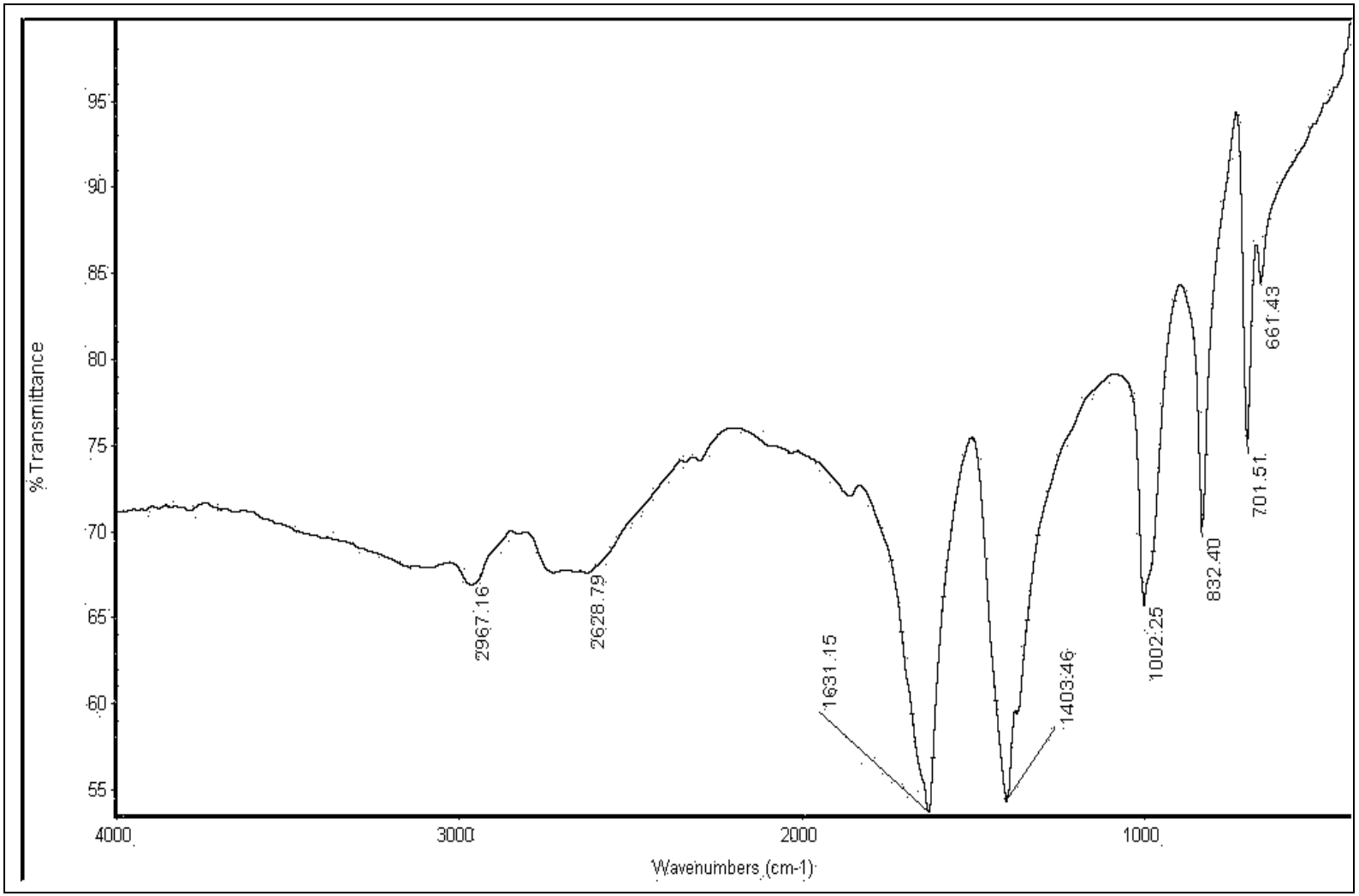

Figure 3.7 FT-IR spectrum of polymer obtained by solution polymerization

3.3 DSC Investigation of Monomer and Polymer of ADCA-K

In order to understand the thermal properties of monomer better, a sample of monomer was heated from room temperature to 200°C. When the heating rate was small, the sample changed color from white to dark brown. When the heating rate was high, the sample puffed at about 120-130°C with evolution of gases. DSC, TGA and Mass spectra were also taken to observe the structural changes.

DSC thermograms of the monomer, after heating up to 120°C and after heating up to 150°C are given in Figures 3.8. In the thermogram of monomer (Figure 3.8a), an exothermic peak is observed at 202.02°C which is due to the evolution of crystal H_2O breaking of CO and CO_2 fragments with a phase change and rearrangement to a new crystal structure. In this case the rate of heating is high (10^0/min) and direct decomposition and structural rearrangement is observed. When the monomer is heated to 120°C in the oven with a slow rate, most of the crystal water is removed and the thermogram (Figure 3.8b) gives a small endothermic peak at 85.89ºC due to the evolution of more H_2O. At 198.47°C, decomposition and rearrangement is observed. The thermogram of sample heated in the oven at a slow heating rate up to 150°C is given in Figure 3.8c. In this thermogram, 3 melting peaks corresponding to different crystalline phases are observed. Therefore, the monomer changes to a polymorphic material at this temperature. These different structures will be investigated further by TGA, NMR, MS and XRD in following sections.

The DSC thermogram of polymer obtained by solid-state polymerization is given in Figure 3.9a. The T_g value of 97.17°C and crystallization peak at 188.58°C are observed. In the thermogram of the polymer obtained from the solution polymerization (Figure 3.9b), the two T_g values are observed at 120.00°C and 131.07°C and a T_m value of 207.62°C. Since the polymerization proceeds by a two-phase process, most probably bimodal polymer (two different average molecular weight) are formed that gives different T_g values, but the same T_m.

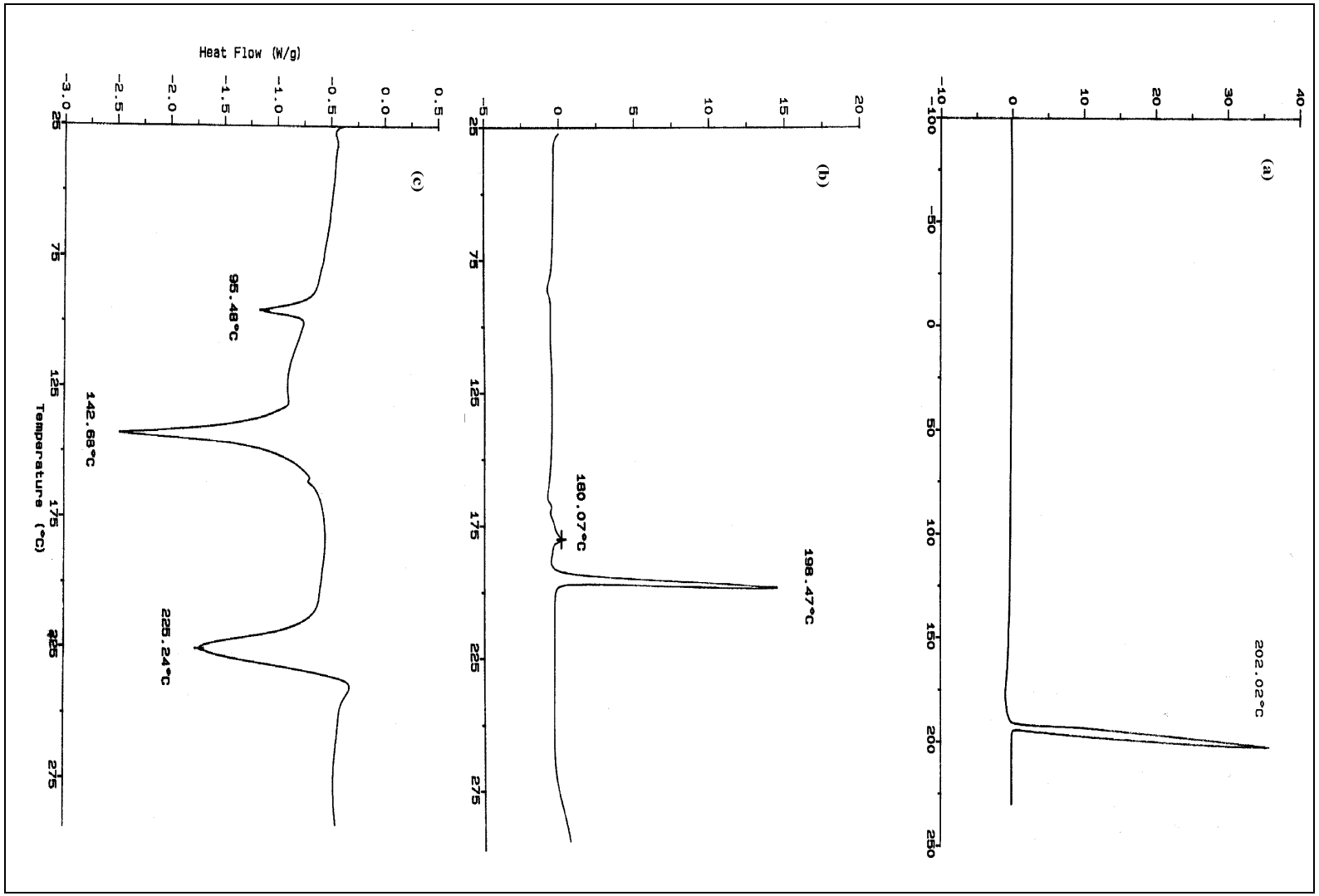

Figure 3.8 DSC thermogram of a) monomer; b) monomer at 120°C; c) monomer at 150°C

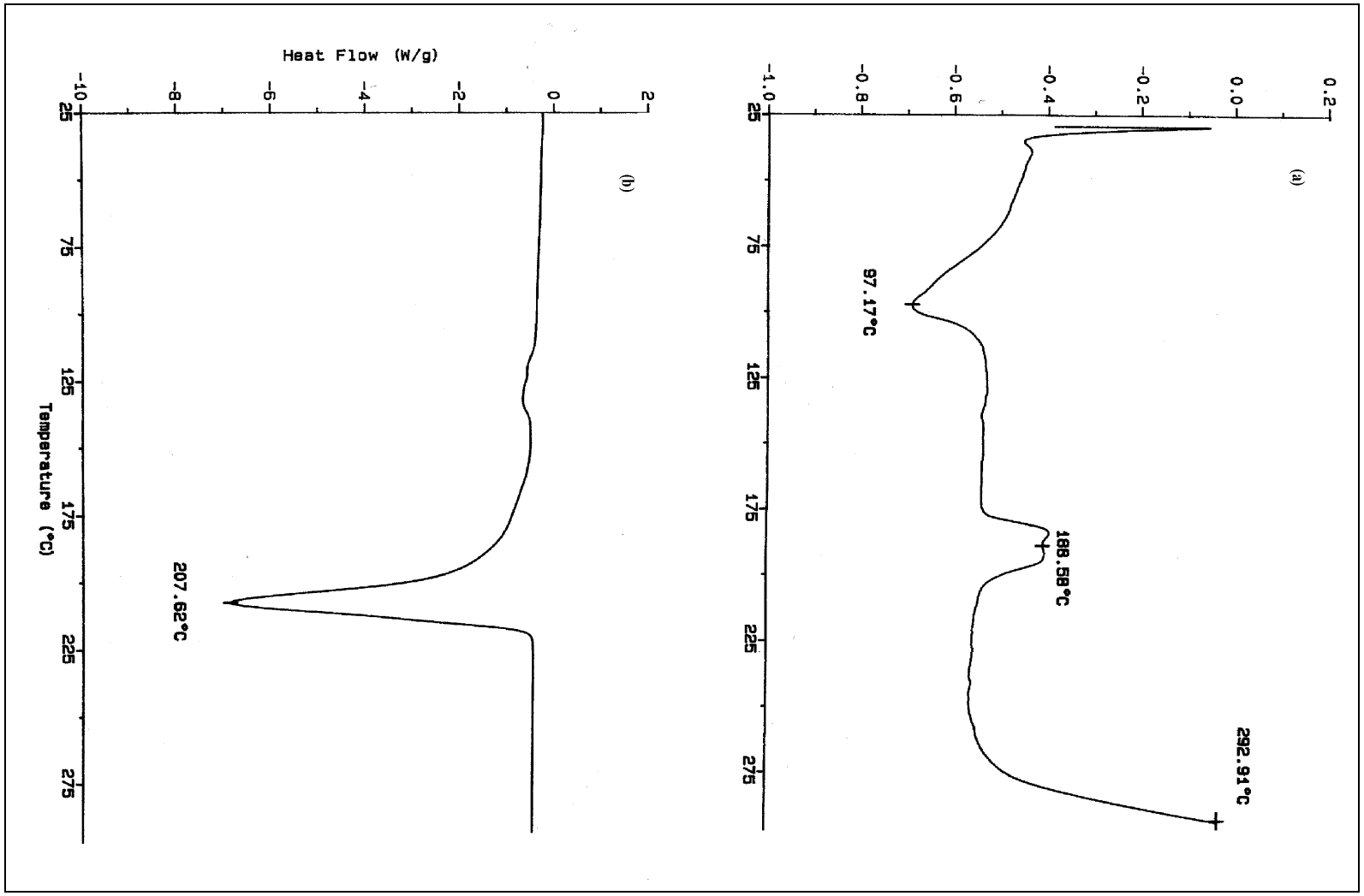

Figure 3.9 DSC thermogram of polymer obtained from a) solid-state polymerization; b) solution polymerization

3.4 Thermal Gravimetric Analysis of Monomer and Polymer of ADCA-K

The TGA thermograms of the monomer and polymer obtained from the solid-state polymerization and solution polymerization are given in Figures 3.10, 3.11 and 3.12, respectively. The corresponding FTIR spectra are also given in the same Figures. The temperature of monomer was increased from room temperature to 90°C with a heating rate of 10^0C and after 90^0C with a rate of 1°C/min in order to prevent the puffing of the samples. In the TGA thermogram of the monomer (Figure 3.10a), the first weight loss starts at about 100ºC and accelerates at 130 ºC. At this stage, the weight loss is about 10 % which corresponds to the evolution of 1 mole of H_2O. That is supported by other findings that monomer contains one mol of the crystal water. Then evolution of CO and CO_2 in addition to H_2O starts at higher temperatures. This is shown in the FTIR spectrum (Figure 3.10b) at 105°C. At about 250^0C, the residual monomer is about 62%.

The TGA thermogram (Figure 3.11a) of the polymer from solid-state polymerization shows that the first weight lost is starting at about 80ºC, and is about 10%. This indicates that 1 mole of crystal water, which is retained in polymer, is evolved. The FTIR spectrum (Figure 3.11b) shows the evolution of H_2O, CO and CO_2. The residual polymer is about 80% at about 470ºC. This indicates that polymer losses some side groups which is probably in the form of CO molecules and cyclization. In the TGA thermogram (Figure 3.12a) of the polymer obtained from solution polymerization, the first weight loss is started at about 60ºC and is 16% indicating that the evolution of absorbed water and solvent. The FTIR spectrum (Figure 3.12b) shows the evolution of H_2O at 60°C and CO_2 at 100°C.

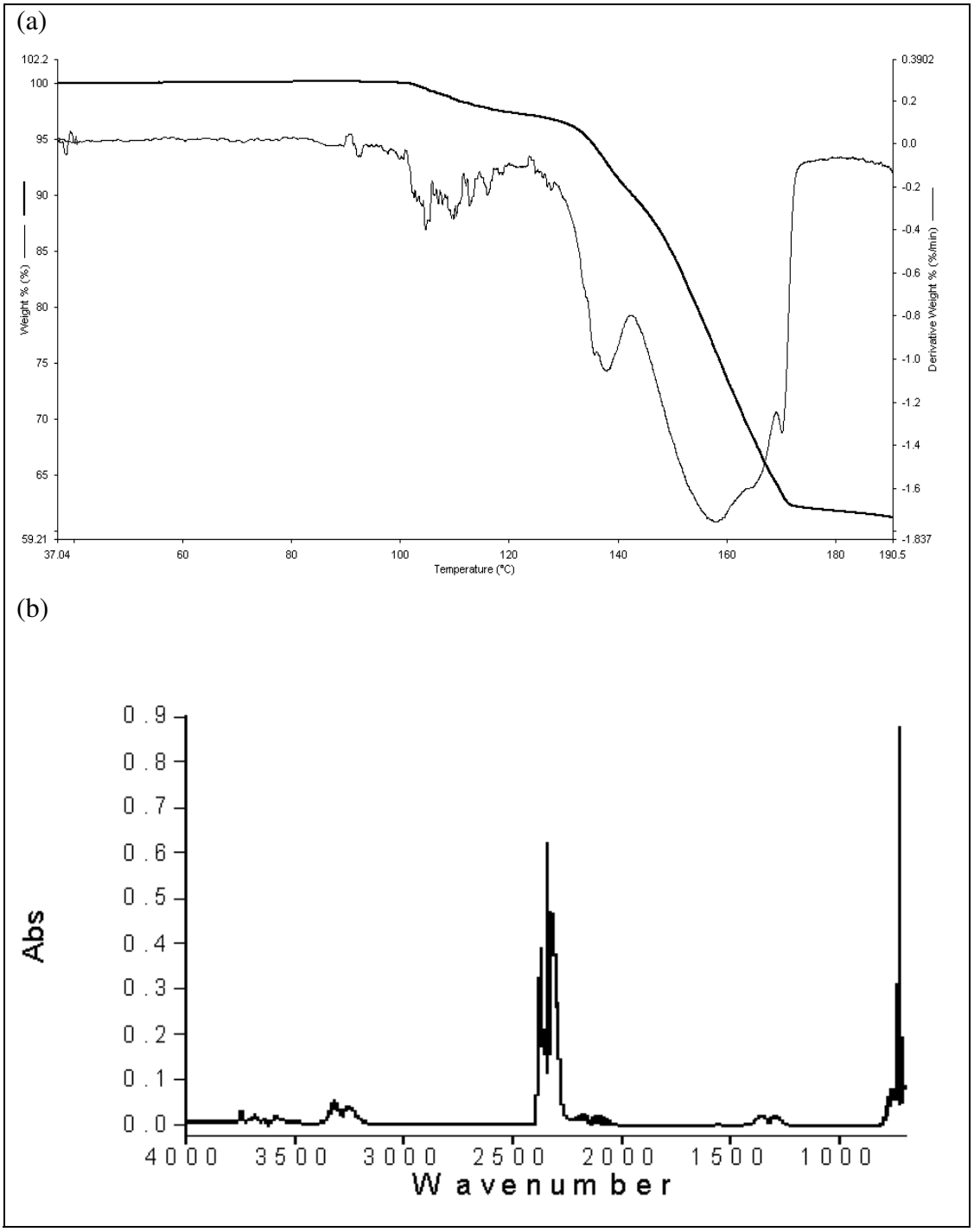

Figure 3.10 a) TGA thermogram; b) FT-IR spectrum of monomer

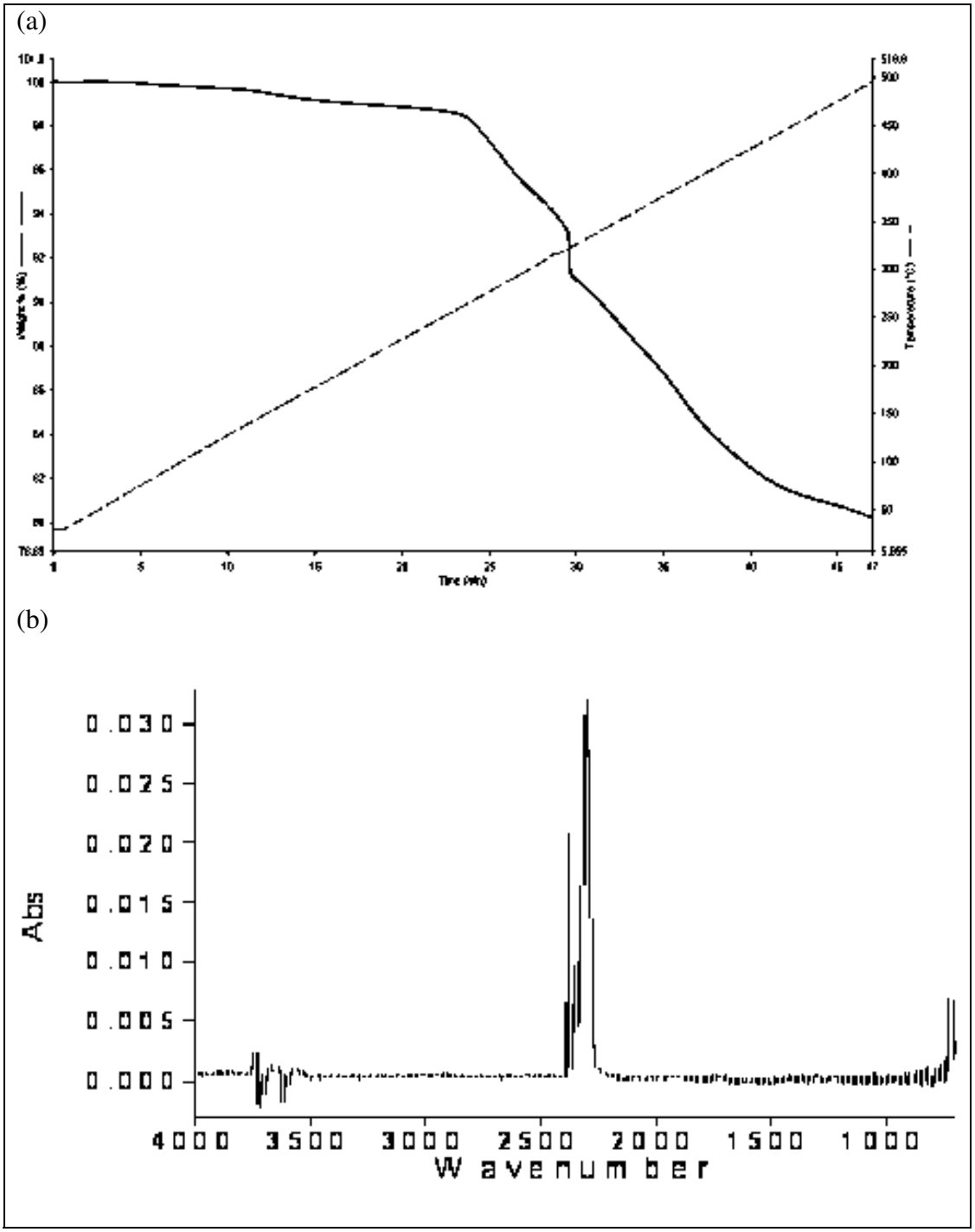

Figure 3.11 a) TGA thermogram; b) FT-IR spectrum of polymer obtained by solid state polymerization

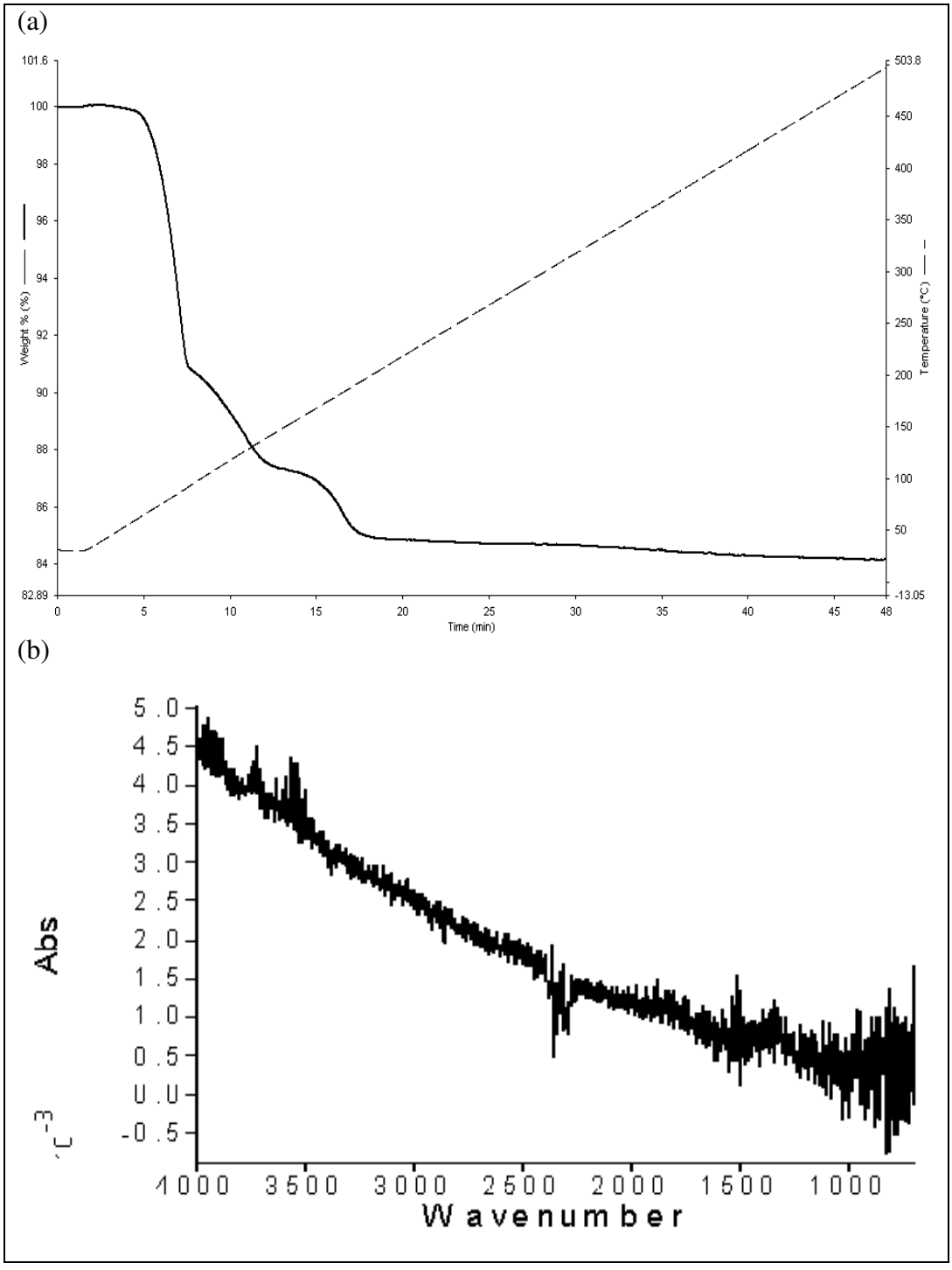

Figure 3.12 a) TGA thermogram; b) FT-IR spectrum of polymer obtained by solution polymerization

3.5 Mass Spectral Investigation

Direct pyrolysis results are used to identify the polymer molecular chain structure and to elucidate the mechanism of polymerization. The mass spectra of monomer and obtained products are given in Figures 3.13-15. The assigned formulas of the most abundant monomer and polymer fragments are shown in Tables 3.5 and 3.6, respectively. The monomer spectrum (Figure 3.13) shows that there is an evolution of some fragments first, then main decomposition maximizing at four temperature zones. The product at different temperatures are given in Figures 3.14 and 3.15. At 50°C (Figure 3.14) the base peak correspond to H_2O (at 18 amu), the peaks at 28 amu and 44 amu represent the CO and CO_2 evolution, respectively. The peaks at 53, 70, 90, 104 and 139 amu are the monomer fragments. They indicate the fragments of cyclic side group. Under thermal and electron beam treatment C≡C bond and side groups cyclization accompanied by the evolution of H_2O, CO and CO_2. The observation of peaks at higher amu values indicates the combinations of fragments and/or the fragmantation of dimer, triplet etc. At higher temperatures (Figure 3.15) the monomer fragmentation and combinations are more dominant.

Table 3.5 Assigned formulas of most abundant monomer fragments under 70 eV

Assigned Formulas	Peak (m/z)	Intensity
H_2O	18	100.00
	28	23.53
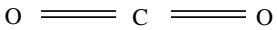	44	92.35
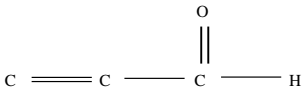	53	82.35
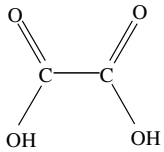	70	50.00
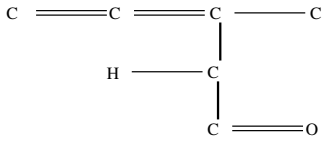	90	20.60
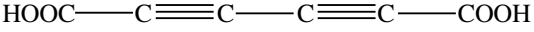	139	53.00
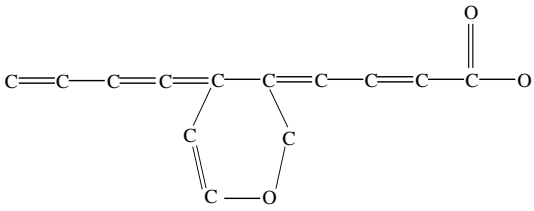	200	9.40

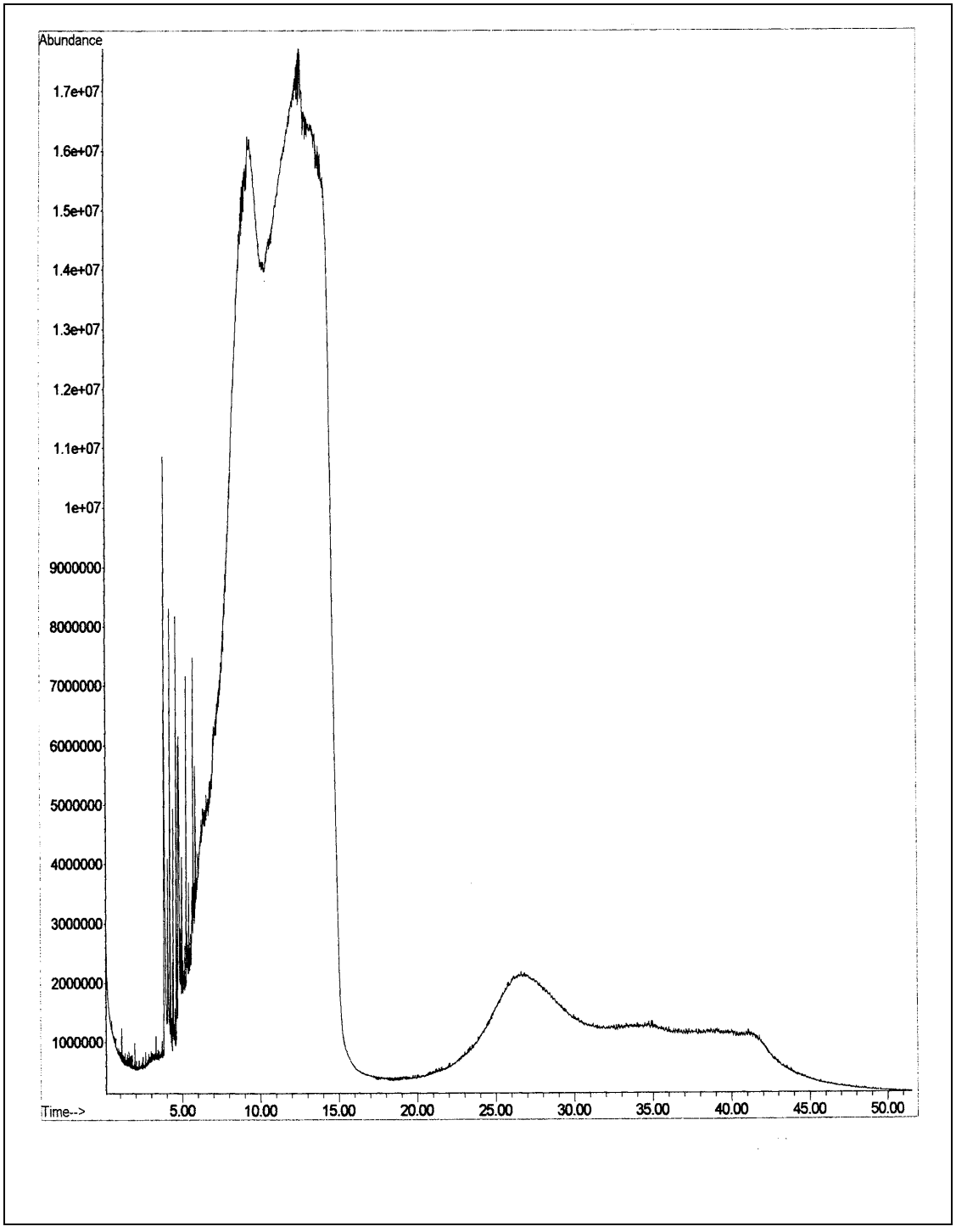

Figure 3.13 Mass spectrum of monomer

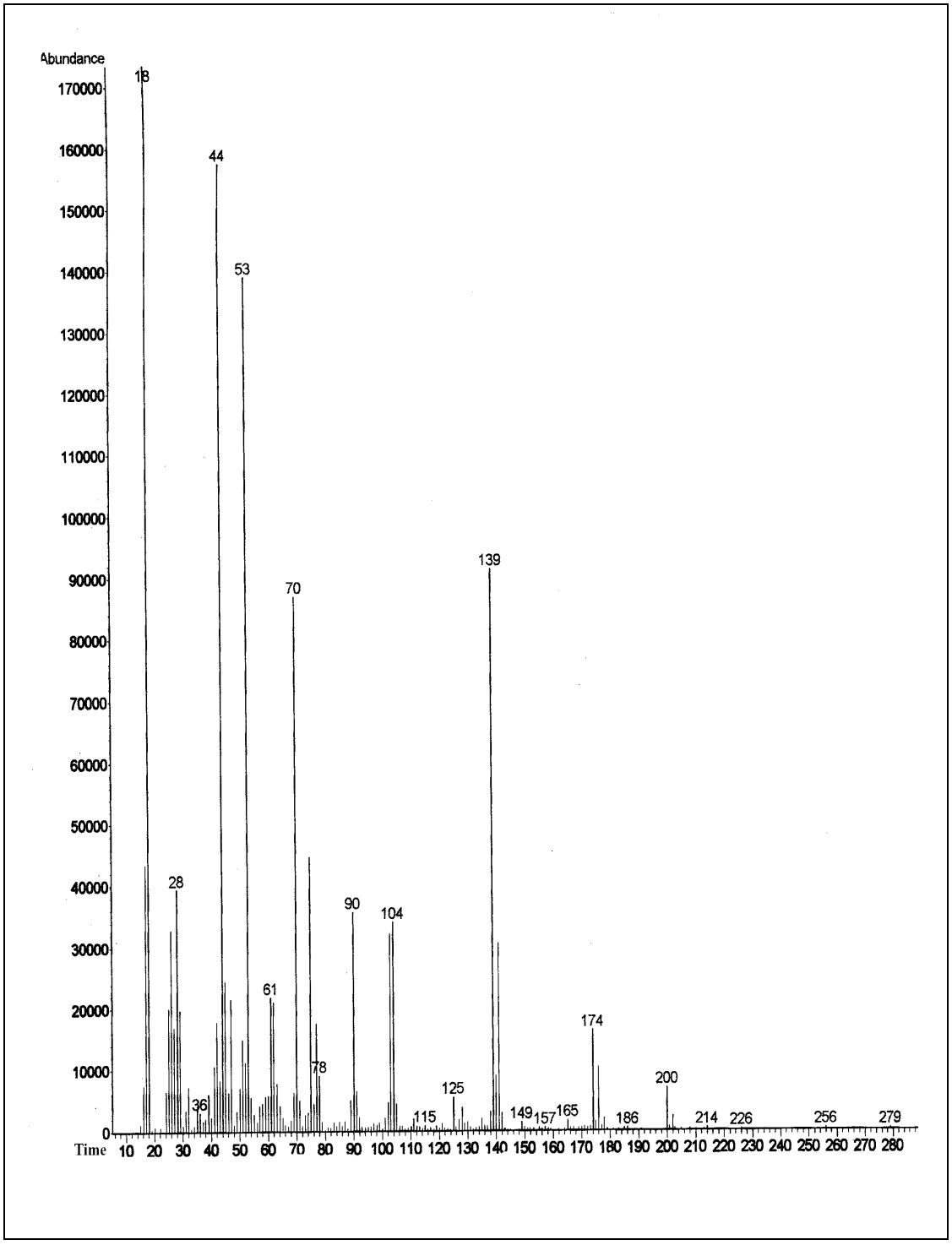

Figure 3.14 Mass spectrum of monomer at 50°C

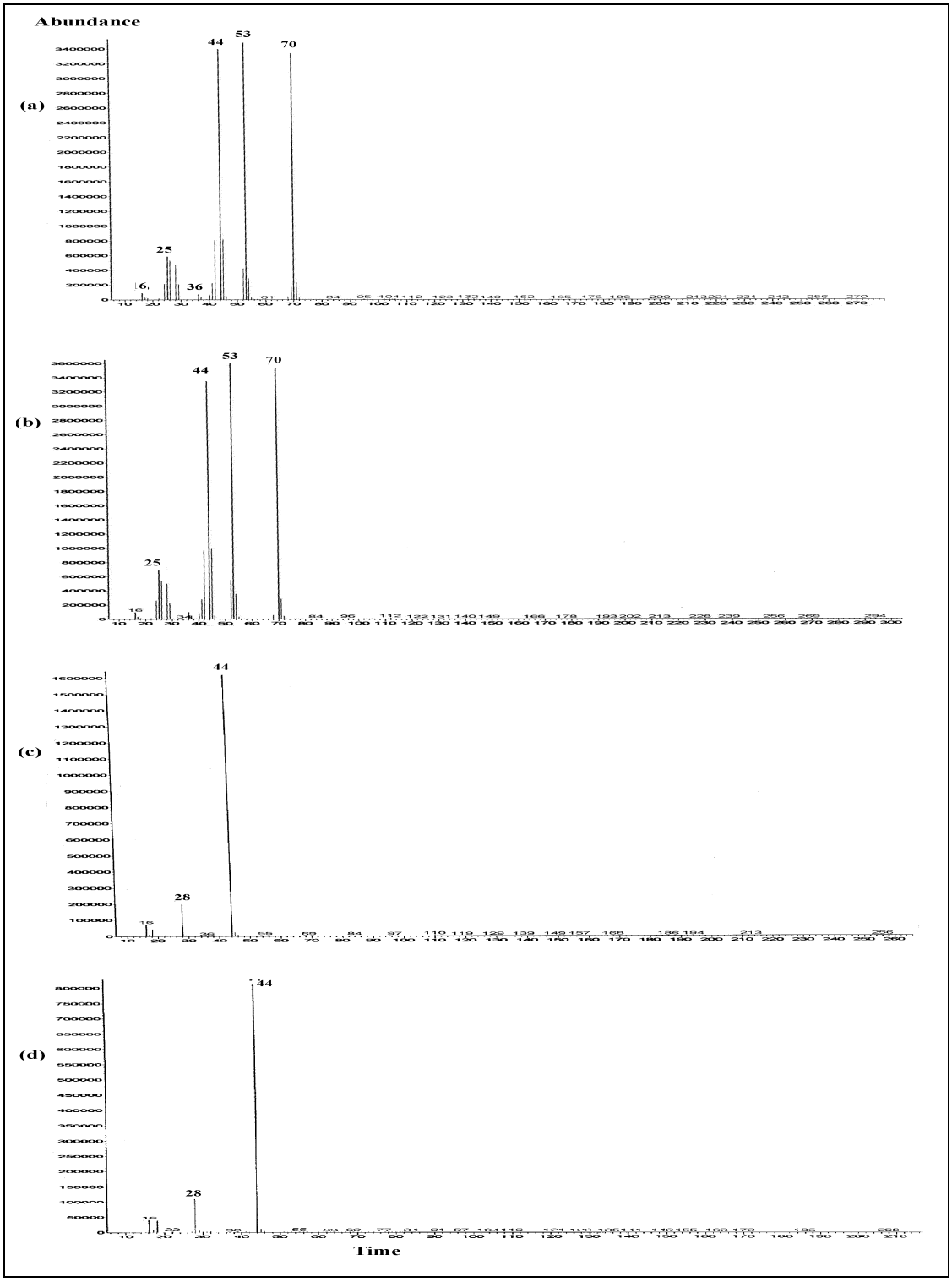

Figure 3.15 Mass spectrum of monomer at a) 95°C; b) 130°C; c) 270°C; d) 410°C

In the mass spectrum of polymer obtained by solid-state polymerization (Figure 3.16), the decomposition is maximized at two temperatures 60°C and 130°C. The base peak at 53 amu represents C=C-COH or C=C-CHO, the other strong peaks are at 70, 44, 18, 139. The corresponding fragments of these and other important peaks are given in Table 3.6. In this spectrum also H_2O evolution in earlier stages of fragmentation is considerable. The intense peak of CO_2 fragments indicate that the COOH side group breaks up mostly as CO_2. These results are also supported in TGA and DSC results.

Table 3.6 Assigned formulas of most abundant polymer fragments under 70 eV

Assigned Formulas	Peak (m/z)	Intensity
H_2O	18	62.50
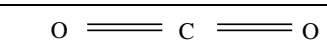	44	76.78
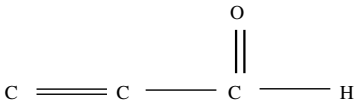	53	100.00
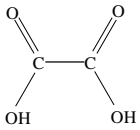	70	85.70
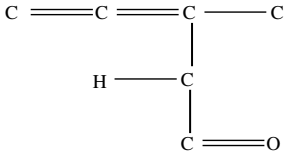	90	23.20
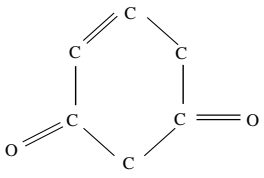	104	12.50
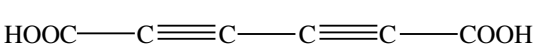	139	41.07
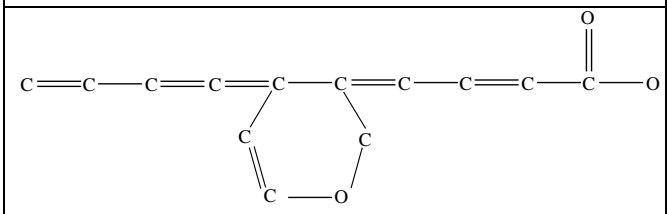	200	3.57

Figure 3.16 Mass spectrum of polymer obtained by solid-state polymerization

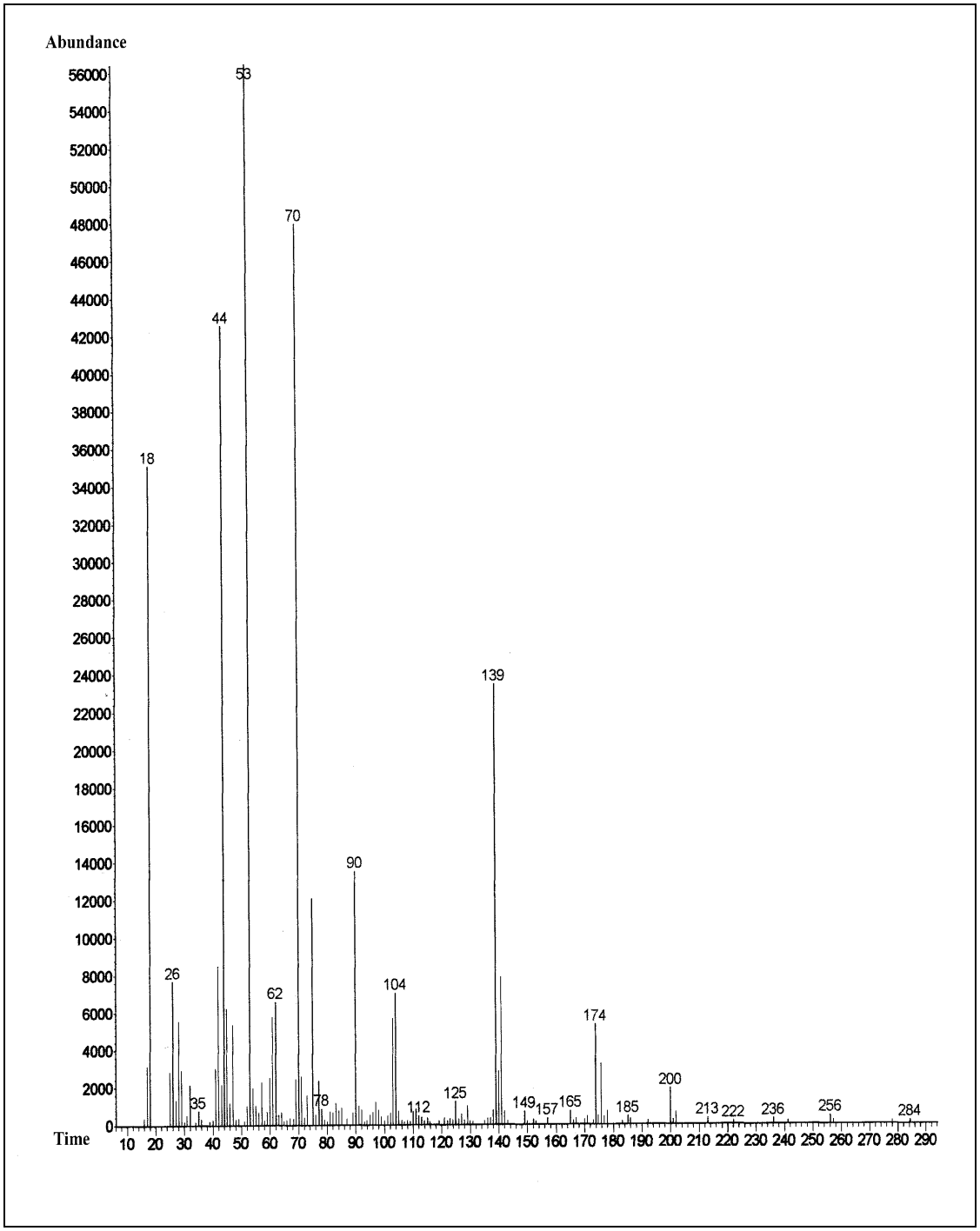

Figure 3.17 Mass spectrum of polymer obtained by solid-state polymerization at 30°C

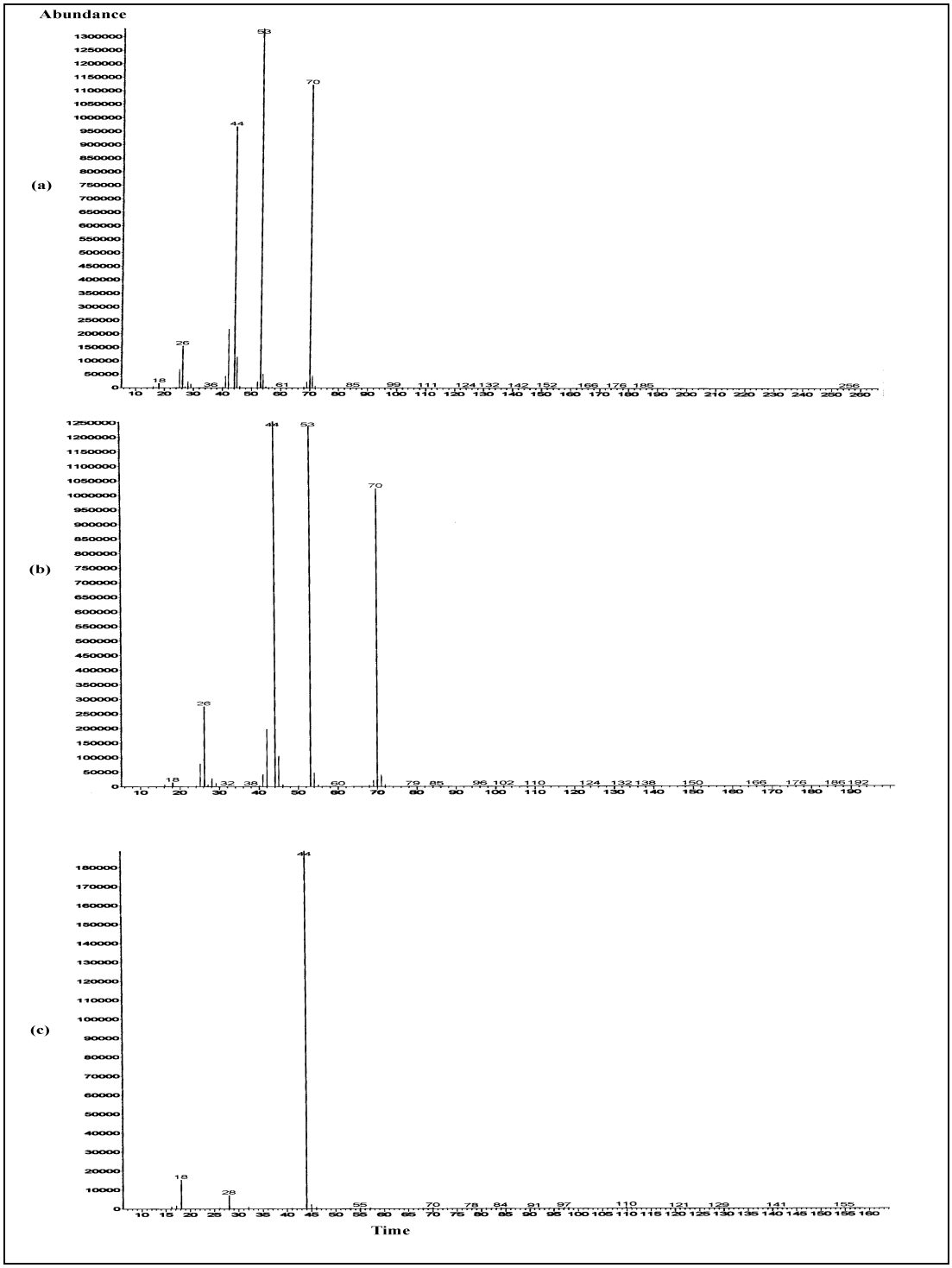

Figure 3.18 Mass spectrum of polymer obtained by solid-state polymerization at a) 67°C; b) 140°C; c) 260°C

3.6 Nuclear Magnetic Resonance (NMR) Analysis

The liquid and solid-state ^{1}H-NMR and ^{13}C-NMR spectra of samples were taken for identification. However, solid-state NMR spectra were similar to that of liquid-state NMR spectra, so the solid-state NMR results are not given for all samples. In the ^{1}H-NMR spectrum of the monomer (Figure 3.19a), an intense peak at 4.6 ppm corresponding to one hydrogen in monomer molecule is observed. When the peak is expanded as given in Figure 3.19b, detailed structure peak is due to the dimerization by hydrogen bonding and crystal water. In the ^{13}C-NMR spectrum of the monomer (Figure 3.19c), the carbonyl C is observed at 160 ppm and C≡C at 75 ppm. Solid-NMR spectrum of monomer gives the same result with some difference in peak shapes. The ^{1}H-NMR spectrum of monomer preheated up to 150°C is given in Figure 3.20a and expanded form in Figure 3.20b. The single hydrogen bond of OH is observed at 4.6 ppm as an intense peak, the other weak peaks are observed in expanded spectrum. They correspond to the rearrangement of structure with evaluation of small fragments as observed from DSC and TGA-FTIR results. In the ^{13}C-NMR spectrum (Figure 3.20c), carbonyl C is observed at 165 ppm and esteric C(O)-**C**-O due to cyclization after splitting of CO and/or CO_2 is observed at 175 ppm. In this case, the triple bond C is not observed which shows the cyclization.

The ^{1}H-NMR and ^{13}C-NMR spectra of the polymers by solid-state and solution polymerization were almost identical and therefore only spectra of polymer samples by solid-state polymerization is given in Figure 3.21. Single intense OH hydrogen is observed at 4.8 ppm and less intense hydrogen peaks are observed in expanded spectrum (Figure 3.21b). These correspond to end group, dimers and cyclic groups. In the ^{13}C-NMR spectrum (Figure 3.21c) of the polymer, carbonyl C is observed at 165 ppm, triple bond C at 85 ppm (as a weak peak) and CH_2 carbon at 40 ppm. These results are in agreement with those of DSC, FT-IR etc. The monomer structure goes through a modification at higher temperatures and when polymerized.

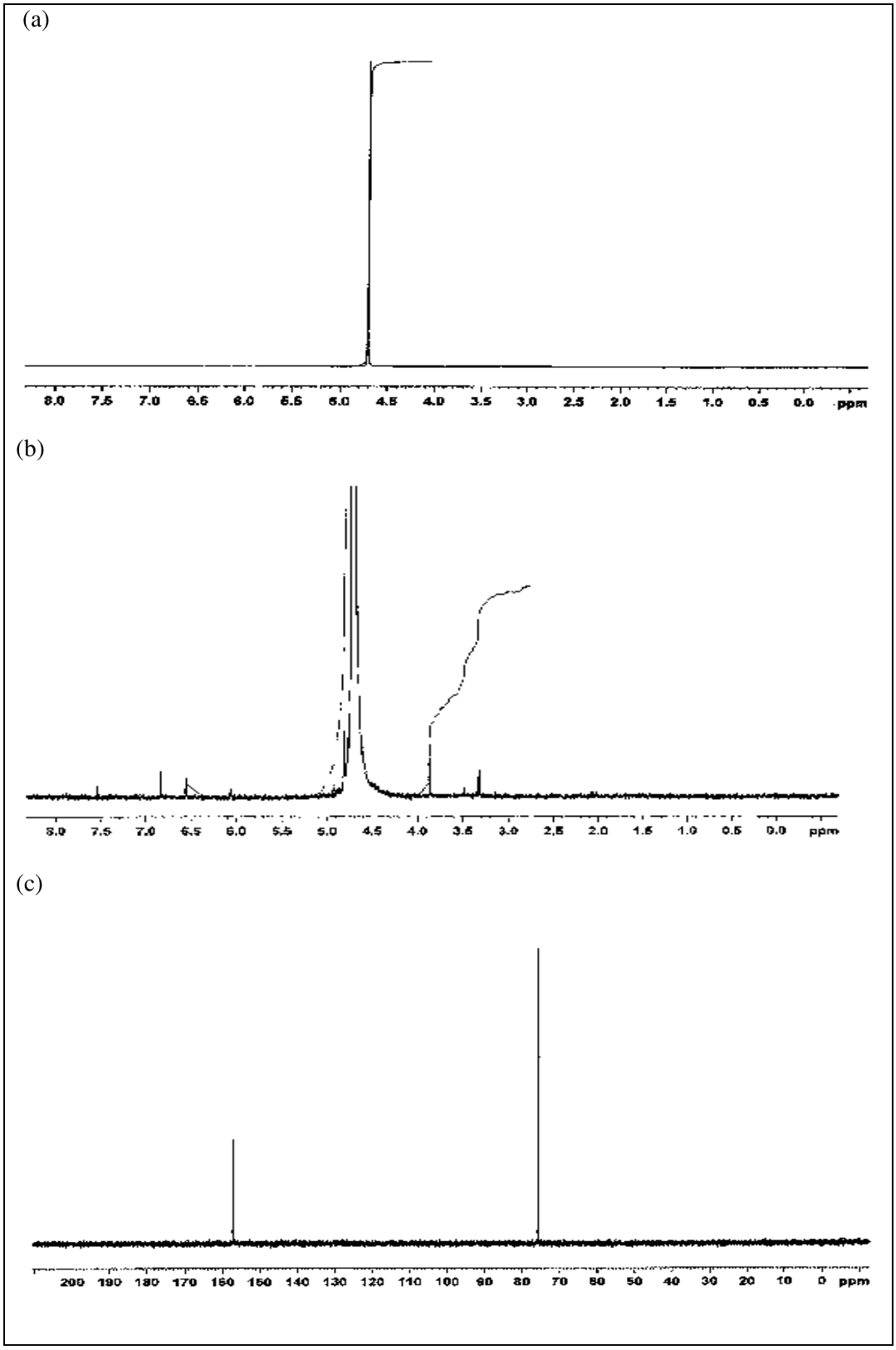

Figure 3.19 a) ^{1}H-NMR spectrum; b) expanded ^{1}H-NMR spectrum; c) ^{13}C-NMR spectrum of monomer

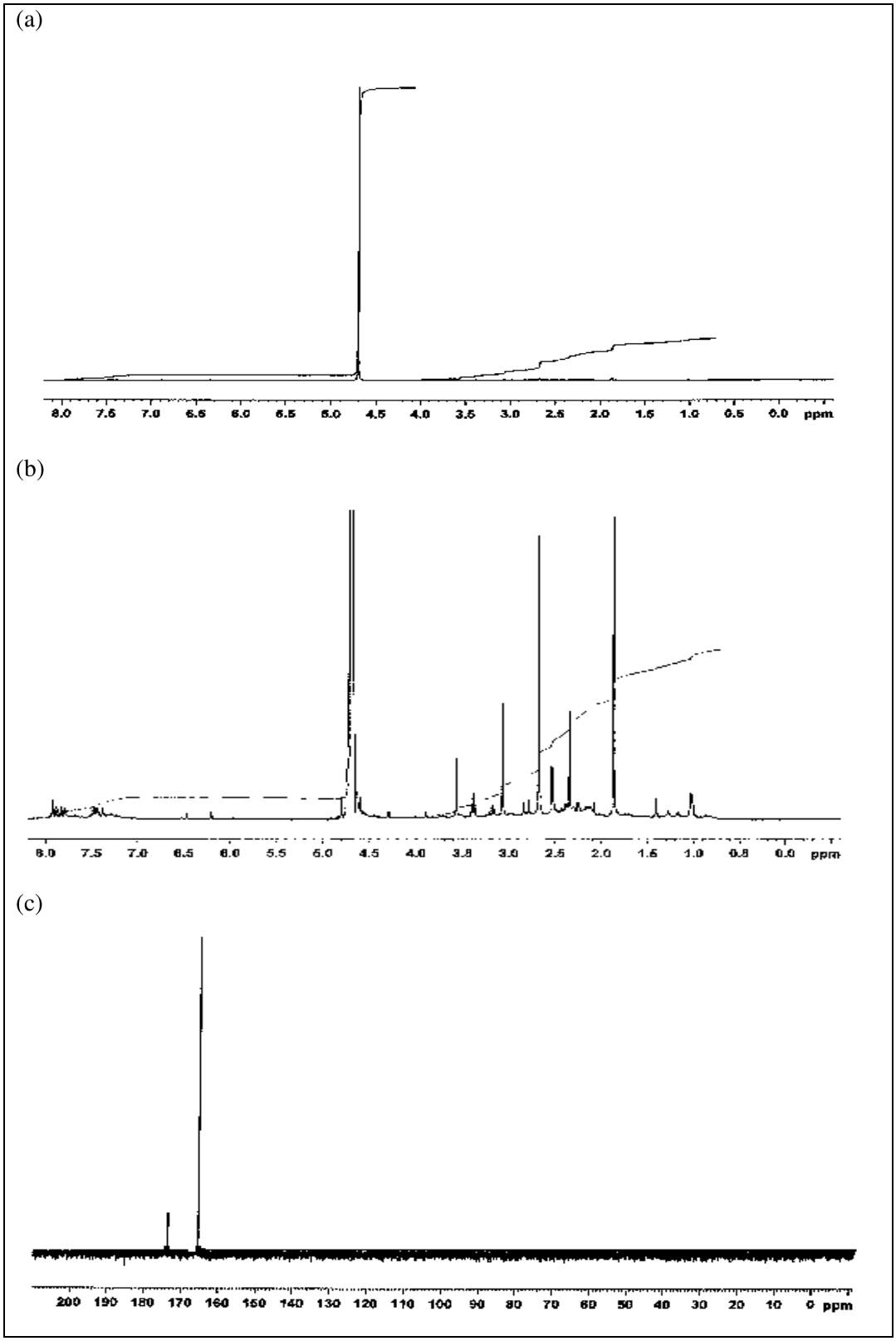

Figure 3.20 a) ^{1}H-NMR spectrum; b) expanded ^{1}H-NMR spectrum; c) ^{13}C-NMR spectrum of monomer at 150ºC

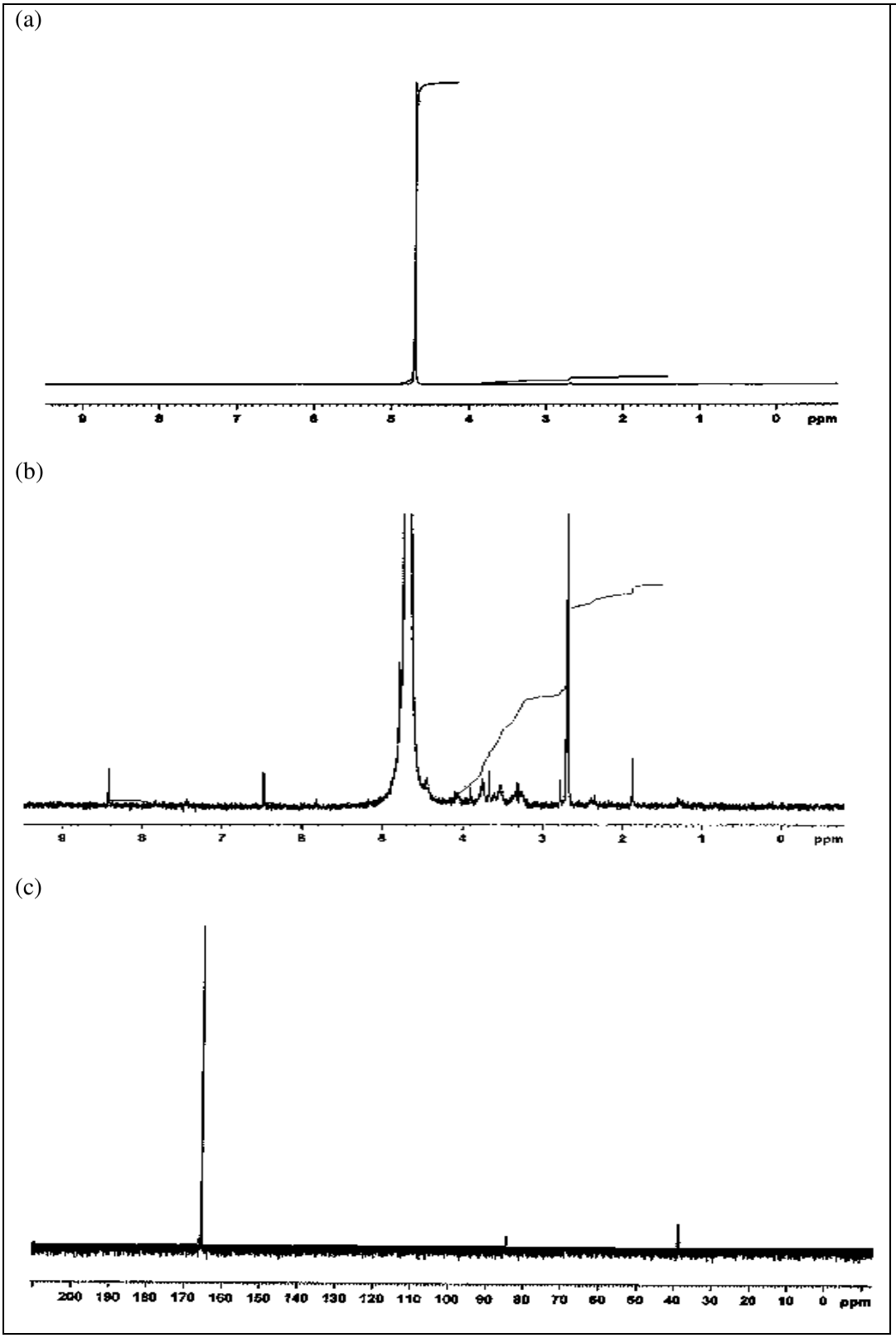

Figure 3.21 a) ^{1}H-NMR spectrum; b) expanded ^{1}H-NMR spectrum; c) ^{13}C-NMR spectrum of polymer

3.7 Structural Investigation by X-Ray method

3.7.1 Monomer Crystal Investigation

The powder X-Ray pattern of ADCA-K is given in Figure 3.22. The Bragg angle θ and relative peak intensities are shown in Table 3.7. The cell parameters and space group are reported by Leban[23]; a= 7.954 Å, b= 11.926 Å, c= 5.918 Å, β= 105.4°, z= 4, space group= C2/c were used for indexing the peaks in powder pattern. The d-spacing values are calculated by a computer program. The calculation and indexing of d-spacing values (d_{obs}) of 50 observed reflections are compared with the calculated values. The indexed hkl indices are also tabulated in Table 3.7. Some of the peaks could not be indexed with these cell parameters. Therefore, other isomorphic structures were tested. The best matching were obtained with cell parameters of ADCA-Rb reported by Blain[24]. The cell parameter of ADCA-Rb are: a= 7.956 Å, b= 12.307 Å, c= 6.216 Å, β =105.6°, z =4, space group =C2/a. Thus, the unmatched hkl indices of the ADCA-K is observed in the ADCA-Rb patterns. That means ADCA-K has two phases of α- and β-structure.

Table 3.7 X-Ray pattern of ADCA-K

θ_{obs}	d^{*2}_{obs}	d^{*2}_{cal}	Possible hkl	I/I_0
6.925	0.02450	0.02403	1 1 0	10
7.525	0.02891	0.02812	0 2 0	8
8.675	0.03834	0.03775	0 1 –1	7
12	0.07286	0.07446	2 0 –1	4
12.8	0.08273	0.08150	2 1 –1	54
13.3	0.08920	0.08732*	0 3 –1*	93
13.75	0.09522	0.09614	2 2 0	100
14.2	0.10142	0.10259	2 2 –1	4
15.075	0.11401	0.11560	1 0 –2	69
15.75	0.12419	0.12288	0 0 –2	45
16.175	0.13080	0.13129	2 3 0	8
16.7	0.13919	0.13774	2 3 –1	5
17	0.14408	0.14373	1 2 –2	29
17.5	0.15241	0.15304	3 0 0	7
18.7	0.17326	0.17548	3 2 –1	46
18.9	0.17685	0.17888	1 3 –2	38
19.1	0.18046	0.18052	2 4 0	16
19.475	0.18735	0.18696	2 4 –1	5
19.875	0.19480	0.19452*	3 0 –2*	9
20.575	0.20816	0.20562	2 3 –2	15
20.75	0.21156	0.21063	3 3 –1	7
21.05	0.21744	0.21632	3 3 0	9
21.6	0.22841	0.22810	1 4 –2	5
22	0.23652	0.23120	3 2 –2	6
22.2	0.24062	0.23955*	1 1 –3*	15

Table 3.7 continued

22.95	0.25627	0.25706	1 0 –3	6
23.25	0.26263	0.26128	4 1 –1	6
23.5	0.26780	0.26640	3 3 –2	9
23.725	0.27286	0.27209	4 0 0	6
24.075	0.28048	0.27912	4 1 0	11
24.35	0.28655	0.28520	1 2 –3	21
24.65	0.29320	0.29780	4 0 –2	5
25.025	0.30160	0.30020	4 2 0	7
25.6	0.31470	0.31560	3 4 –2	5
26.275	0.33030	0.32600	4 2 –2	6
26.55	0.33677	0.33534	4 3 0	5
26.775	0.34207	0.34840	3 2 –3	13
27.125	0.35038	0.35450*	2 4 –3*	9
27.5	0.35938	0.35912*	4 4 –1*	7
28.25	0.37763	0.37812*	4 4 0*	11
29.05	0.39740	0.39592*	4 4 –2*	11
29.625	0.41186	0.41000	4 4 –2	7
30.025	0.42204	0.42311*	1 1 –4*	6
30.55	0.43545	0.43276	3 4 –3	7
30.875	0.44385	0.44292*	1 2 –4*	4
31.25	0.45359	0.45996	1 0 –4	6
31.825	0.46868	0.46699	1 1 –4	4
32.275	0.48058	0.48800	1 2 –4	4

* these data indexed with respect to ADCA-Rb pattern

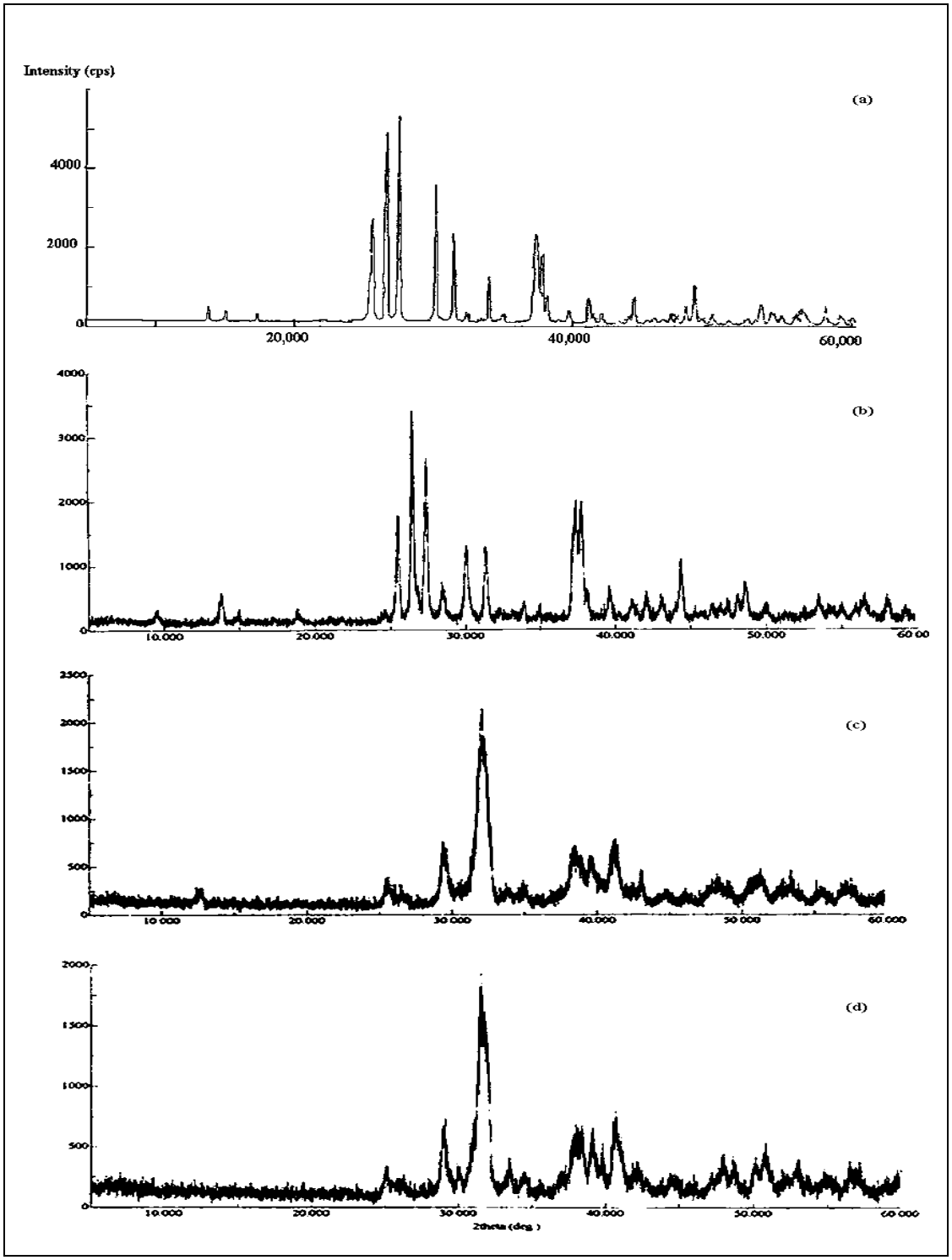

Figure 3.22 X-Ray spectrum of a) monomer; b) at 120°C; c) at 150°C; d) at 190°C

The X-Ray powder patterns of ADCA-K preheated up to temperatures of 120, 150 and 190°C are also given in Figure 3.22. The X-ray pattern of monomer (Figure 3.22b) preheated shows some differences to that of Figure 3.22a. After the d-spacing calculation and indexing for observed reflections (Figure 3.22b), hkl indices are tabulated in Table 3.8. The X-Ray powder pattern of ADCA-K at 120, 130, 140° show same spectra. But at 150°C (Figure 3.22c), due to the structural rearrangement after fragmentation (as observed by DSC thermogram) the X-ray pattern is much changed compared to the one in Figures 3.22a and 3.22b. The possible hkl indices and d-spacing values are given in Table 3.9. In the spectrum of monomer preheated up to 190°C as given in Figure 3.22d, it is very similar to the pattern in Figure 3.22c. The possible hkl indices and d spacing values are given in Table 3.10. Since all X-ray patterns could be indexed with the same cell parameters, the structural changes with temperature takes place by a topotactic mechanism.

Table 3.8 X-Ray pattern of ADCA-K at 120°C

θobs	d^{*2}_{obs}	d^{*2}_{cal}	**Possible hkl**	**I/I0**
6.935	0.02426	0.02403	1 1 0	15
9.435	0.04529	0.04513	1 2 0	11
12.775	0.08241	0.08150	2 1 -1	53
13.255	0.08861	0.08732*	0 3 -1*	100
13.715	0.09474	0.09399	0 3 -1	80
14.23	0.10184	0.10259	2 2 -1	23
15.045	0.11357	0.11249	0 4 0	39
15.695	0.12334	0.12288	0 0 -2	37
16.945	0.14318	0.14320	0 4 -1	13
18.7	0.17326	0.17050	2 2 -2	59
18.83	0.17558	0.17547	3 2 -1	49
18.875	0.17639	0.17888	1 3 -2	59
19.795	0.19331	0.19224*	2 3 -2*	19
19.84	0.19415	0.19452*	3 0 -2*	19
21.015	0.21676	0.216315	3 3 0	18
22.175	0.24010	0.23537	0 4 -2	33
24.27	0.28478	0.28520	1 2 -3	22

* these data indexed with respect to ADCA-Rb pattern

Table 3.9 X-Ray pattern of ADCA-K at 150°C

θobs	d^{*2}_{obs}	d^{*2}_{cal}	**Possible hkl**	**I/I0**
6.26	0.02004	0.02403	1 1 0	12
12.805	0.08279	0.08150	2 1 -1	19
14.685	0.10832	0.11249	0 4 0	36
16.045	0.12876	0.12288	0 0 -2	100
19.225	0.18275	0.18696	2 4 -1	34
19.785	0.19311	0.19452*	3 0 -2*	25
20.63	0.20923	0.21012	3 1 -2	34
21.525	0.22691	0.22810	1 4 -2	23
25.65	0.31583	0.31560	3 4 -2	23

* these data indexed with respect to ADCA-Rb pattern

Table 3.10 X-Ray pattern of ADCA-K at 190°C

θobs	d^{*2}_{obs}	d^{*2}_{cal}	**Possible hkl**	**I/I0**
12.525	0.07927	0.08030	1 3 0	18
14.49	0.10552	0.10259	2 2 –1	36
14.56	0.10652	0.10564*	0 4 0*	39
14.955	0.11225	0.11249	0 4 0	20
15.735	0.12396	0.12288	0 0 –2	95
15.765	0.12442	0.12267*	1 4 0*	100
15.9	0.12650	0.12950	1 4 0	85
16.725	0.13958	0.13774	2 3 –1	22
17.22	0.14772	0.14735	3 0 –1	16
18.92	0.17721	0.75475	3 2 –1	32
19.01	0.17883	0.17888	1 3 –2	36
19.2	0.18229	0.18117	3 2 0	36
19.565	0.18902	0.18696	2 4 –1	35
19.59	0.19537	0.19224*	2 3 -2*	28
20.255	0.20201	0.20113*	3 1 -2*	38
20.35	0.20384	0.20310	3 0 -2	42
21.055	0.21755	021632	3 3 0	21
22.205	0.24074	0.24887*	2 0 -3*	16
24.005	0.27894	0.27870	2 1 –3	24
24.325	0.28597	0.28520	1 2 –3	23
25.435	0.31092	0.31560	3 4 –2	28
26.54	0.33649	0.33534	4 3 0	20
28.305	0.37898	0.37812*	4 4 0*	21
28.63	0.38699	0.38456	4 4 0	20

3.7.2 Polymer Crystal Investigation

The X-Ray spectrum of polymer obtained from solid-state polymerization and solution polymerization are given in Figure 3.23 and 3.24, respectively. In the X-Ray Spectrum of polymer obtained from solid-state polymerization, it can be seen that the polymer has high crystallinity. The indexing were carried out with cell parameters of ADCA-K and ADCA-Rb. The results are tabulated in Table 3.11: Since the X-ray crystal structure of monomer and polymer are similar, polymerization takes place by a topotactic mechanism. In the X-Ray Spectrum of polymer obtained from solution polymerization (Figure 3.24), polymer is highly crystalline, but not as much as that obtained from solid-state polymerization. The obtained reflection could still be indexed with cell parameters of monomer. Therefore, the polymerization mechanism is a topotactic one. The results of indexing are tabulated in Table 3.12.

Table 3.11 X-Ray pattern of polymer obtained from solid-state polymerization

θobs	d^{*2}_{obs}	d^{*2}_{cal}	**Possible hkl**	**I/I0**
7.725	0.03045	0.03046	0 0 -1	10
9.25	0.04355	0.42620	1 1 -1	48
10.35	0.05440	0.05431*	0 2 -1*	21
10.725	0.05837	0.05880	0 2 -1	20
13.525	0.09219	0.09399	0 3 -1	27
13.75	0.09523	0.09614	2 2 0	15
14.975	0.11254	0.11249	0 4 0	100
15.625	0.12227	0.12260	1 1 -2	49
15.9	0.12650	0.12754*	2 3 0*	24
17.6	0.15410	0.15440	3 1 -1	52
18.825	0.17549	0.17550	3 2 -1	57
19.975	0.19669	0.19452*	3 0 -2*	36
20.475	0.20624	0.20560	2 3 -2	14
21.175	0.21992	0.22093*	3 2 -2*	16
21.4	0.22440	0.22810	1 4 -2	37
22.35	0.24472	0.24887*	2 0 -3*	24
23.1	0.25946	0.25985	3 4 -1	14
24.05	0.27995	0.27912	4 1 0	23
24.35	0.28655	0.28520	1 2 -3	18
26.325	0.33148	0.32600	4 2 -2	17
26.45	0.33440	0.33490	2 3 -3	17
26.85	0.34383	0.34840	3 2 -3	10
27.55	0.36059	0.36113	4 3 -2	17

* these data indexed with respect to ADCA-Rb pattern

Table 3.12 X-Ray pattern of polymer obtained from solution polymerization

θobs	d^{*2}_{obs}	d^{*2}_{cal}	**Possible hkl**	**I/I0**
15.55	0.12113	0.12260	1 1 -2	100
19.10	0.18047	0.18052	2 4 0	49
20.20	0.20096	0.20310	3 0 -2	43
21.65	0.22942	0.22810	1 4 -2	25
22.20	0.24063	0.23955*	1 1 -3*	43
22.70	0.25101	0.25425	4 0 -1	25
25.00	0.30104	0.30020	4 2 0	34
27.50	0.35937	0.35912*	4 4 -1*	38
27.55	0.36142	0 36113	4 3 -2	35
27.6	0.36179	0.36670	4 4 -1	32

* these data indexed with respect to ADCA-Rb pattern

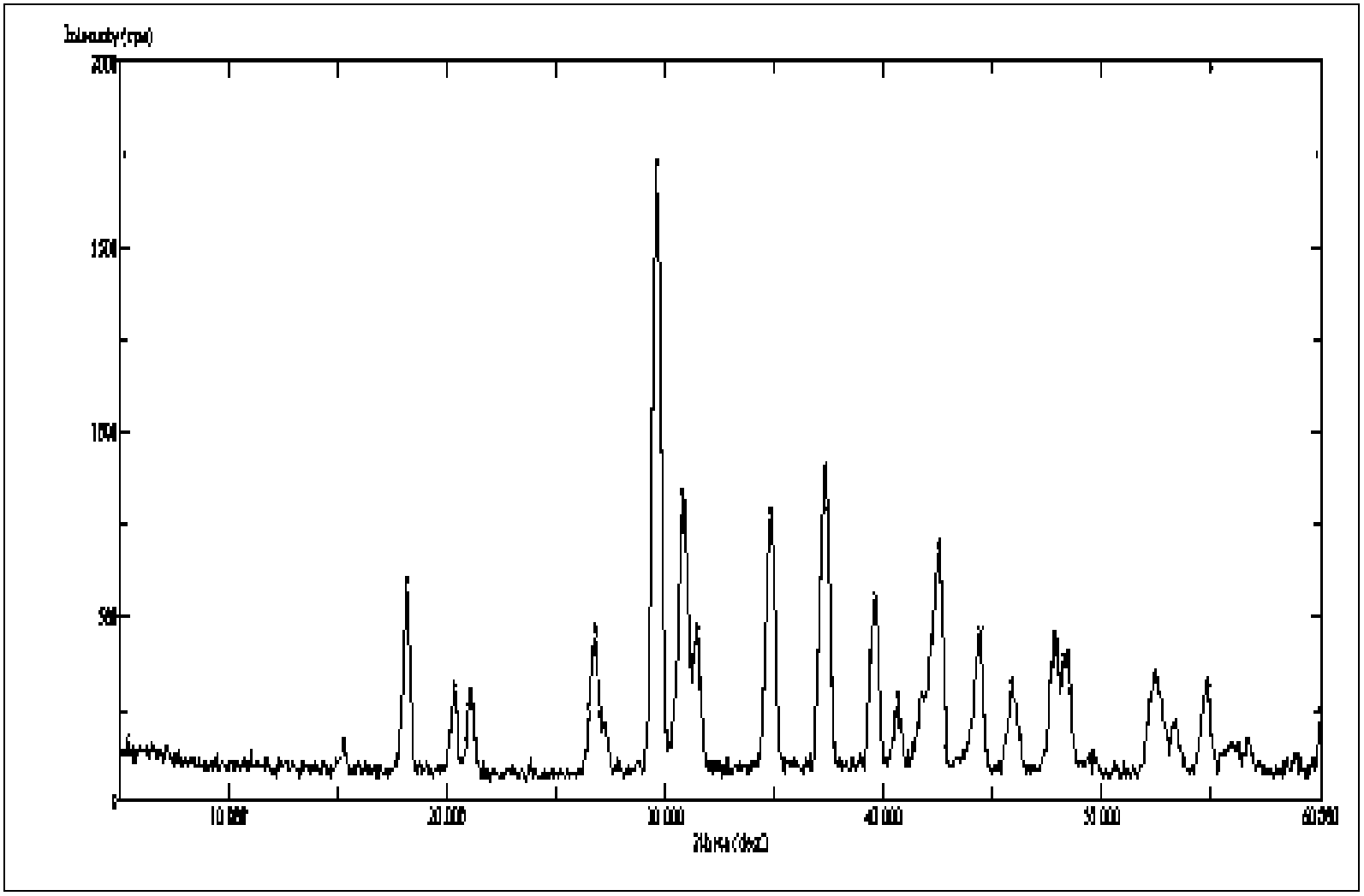

Figure 3.23 X-Ray spectrum of polymer obtained by solid-state polymerization

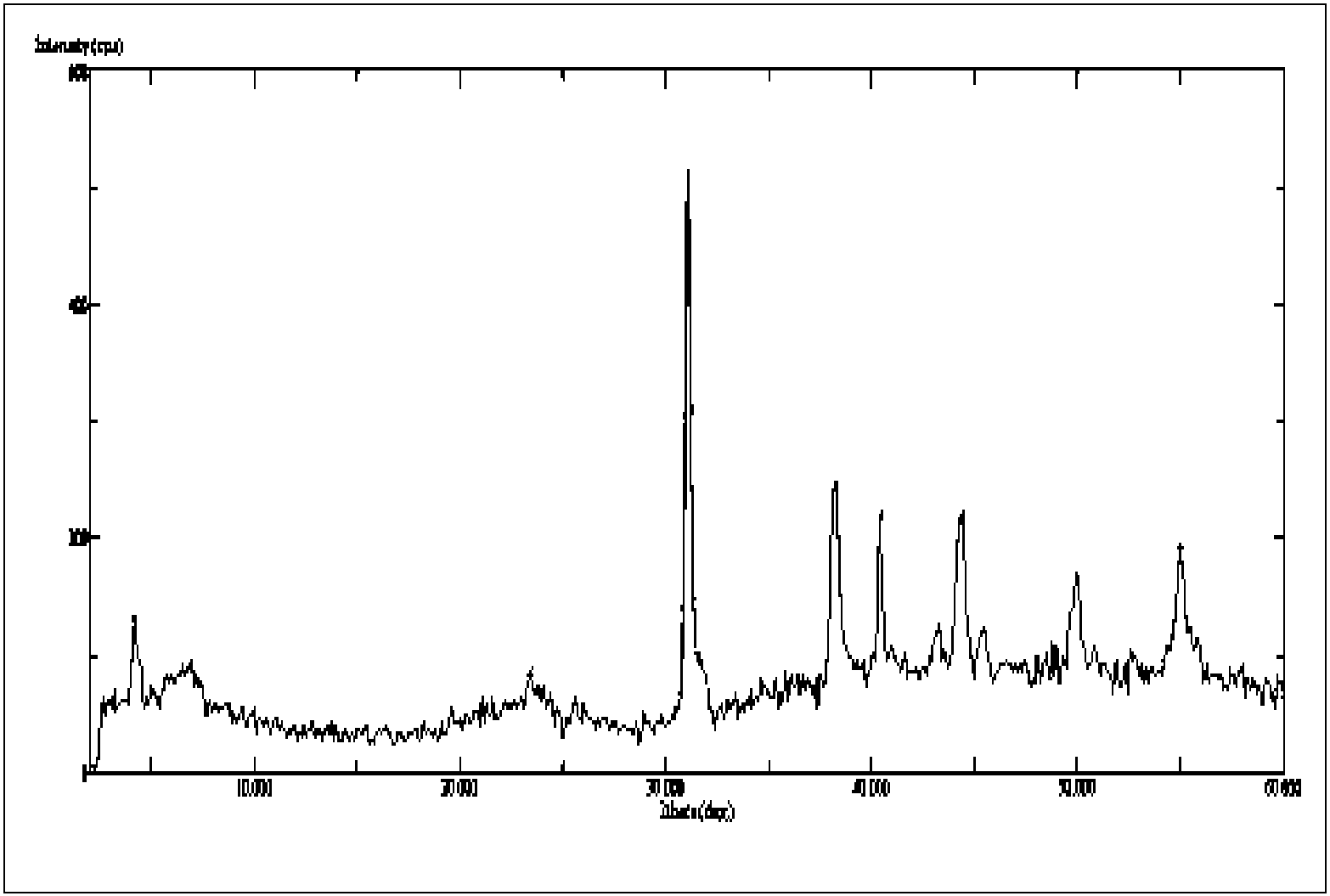

Figure 3.24 X-Ray spectrum of polymer obtained by solution polymerization

CHAPTER 4

CONCLUSION

The following conclusions can be mentioned:

1. ADCA-K can be polymerized by both radiation induced solid-state polymerization and chemical initiator induced solution polymerization.
2. The structure of monomer is linear with carbon in sp hybridization form therefore polymerization cannot proceed easily because of steric hindrance.
3. The heating of monomer results in evolution of H_2O, CO and CO_2 with a drastic change in the structure of monomer which is shown by FT-IR, DSC and MS investigations.
4. Monomer polymerization by radiation takes place at high radiation doses. This is because the initial energy given is used to disturb the lattice structure and bring the monomer to a suitable Van der Waals distances for combination. At this time, the hybrid form of C may also change.
5. The gas evolutions could also be observed from TGA results and the TGA also showed that more than 80% of polymer is resistant to temperature higher than 500°C.
6. X-Ray results show that polymer obtained is highly crystalline and polymerization mechanism is topotactic.

REFERENCES

1. Usanmaz, A., Melad O. K., J. Polym. Sci. Part A: Polym. Chem. 34, 1087, 1996

2. Adler, G., Ballatine, D.S., and Baysal, B., J. Polym. Sci. 48, 198, 1954

3. Enkelman, V., Adv. Polym. Sci. 63, 91, 1984

4. Usanmaz, A., Tr. J. of Chem. 21, 304, 1997

5. Wegner, G., Macromol. Chem. 145, 85, 1971

6. Aoki, K., Usuba, S., Yoshida, M., Kakudate, Y., Tanaka, K., and Fujiwara, S., J. Chem. Phys. 89, 1, 1988

7. Trout, C.C., and Badding, J.V., J. Phys. Chem. A 104 ,8142, 2000

8. Hirchfeld, F.L., and Schmidt, Y., J. Polym. Sci. B5, 813, 1967

9. Keller, A., and Matusiak, R., J. Mol. Catalysis A: Chemical 142, 317, 1999

10. Kubo, H., Hayano, S., and Masuda, T., J. Polym. Sci.Part A: Polym. Chem. 38, 2697, 2000

11. Xu, K., Peng, H., and Tang, Z.B., Macromolecules 33, 6918, 2000

12. Niki, A., Masuda, T., and Higashimura, T., J. Polym. Sci. Part A: Polym. Chem. 25, 1553, 1987

13. Masuda, T., Kawai, M. ,and Higashimura, T., Polymer 23, 744, 1982

14. Yamaguchi, I., and Osakada, K., Inorganica Chimica Acta 220, 35, 1994

15. Leiserowitz, L., Acta Cryst. B32, 775, 1976

16. Benghiat, V., Leiserowitz, L., and Schmidt, G.M.J., J. Chem. Soc. Perkin II, 1769, 1972

17. Usanmaz, A.and Altürk, E., J. Macromol. Sci.-Pure Appl. Chem. A39, 379, 2002

18. Cataldo, F., Croatica Chemica Acta 73, 435, 2000

19. Allan, J.R., Beaumont, P.C., Macindoe, L., Milburn, G.H.W., and Werninck, A., Thermochimica Acta 117, 51, 1987

20. Mattes, R., and Plescher, G., Acta Cryst. B37, 697, 1981

21. Kalsbeek, N., Schaumburg, K., and Larsen, S., J. Mol. Struct. 299, 155, 1993

22. Gupta, M.P., and Mahat, A.P., Indian J. Phys. 49, 950, 1975

23. Leban, I., Golic, L., and Speakman, J.C., J. Chem. Soc. Perkin II, 703, 1973

24. Blain, J., Speakman, J.C., Stamp, L.A., Golic, L. And Leban, I., J. Chem. Soc. Perkin II, 706, 1973

25. Hohn, F., Pantenburg, I., and Rushewitz, U., Chem. Eur. J. 2002, 8,4536

26. Pantenburg, I., and Ruchewitz, U., Z. Anorg. Allg. Chem. 2002, 628, 1697

27. Ruchewitz, U., and Paantenburg, I., Acta Cryst. C-Cryst. Struc. Comm. 2002, 58, m483.

28. Skoulika, S., Chem. Mater. 2003, 15, 4576.

29. Billetter, H., Hohn, F., Pantenburg, I., and Rushewitz, U., Acta Cryst. C-Cryst. Struc. Comm. 2003, 59, m130.

30. Ruschewitz, U., Hohn, F., Billetter, H., and Pantenburg, I., Zeitschrift fur Naturforschung Section B-A jornal of Chem. Sci. 57, 1375, 2002

31. Leban, I., and Rupnik, A., Acta Cryst. C-Cryst. Struc.Comm. 1992, 48, 821.

32. McCormick, B. J., Synthetic Metals 2001, 120, 969.

33. Sekikawa, T., Miyakubo, K., Takeda, S., and Kobayashi, T., J. Phys. Chem. 1996, 100, 5844

34. Miyakubo, K., and Nakamura, N., Z. Naturforsch. 2002, 57 a, 337